PARAMETRIC INSTABILITIES IN INHOMOGENEOUS PLASMA

Contents

PARAMETRIC INSTABILITIES IN INHOMOGENEOUS PLASMA*

Dwight Roy Nicholson

Lawrence Berkeley Laboratory
University of California
Berkeley, California 94720

June 6, 1975

ABSTRACT

We consider the nonlinear coupling of three waves in a plasma. One of the waves is assumed large and constant; its amplitude is the parameter of the parametric instability. The spatial-temporal evolution of the other two waves is treated theoretically, in one dimension, by analytic methods and by direct numerical integration of the basic equations. Various monotonic forms of inhomogeneity are considered; agreement with previous work is found and new results are established. Nonmonotonic inhomogeneities are considered, in the form of turbulence and, as a model problem, in the form of a simple sinusoidal modulation. Relatively small amounts of nonmonotonic inhomogeneity, in the presence of a linear density gradient, are found to destabilize the well-known convective saturation, absolute growth occurring instead.

---

* This work was supported by the U. S. Energy Research and Development Administration.

I. GENERAL CONSIDERATIONS AND MONOTONIC INHOMOGENEITIES

A. Introduction

The three wave coupled mode equations are encountered in many branches of physics. In solid state physics, an electromagnetic driver can couple an electronic disturbance and another electromagnetic wave, the process being called Raman scattering[1-3]; replace the electronic disturbance by an ion lattice vibration and we have Brillouin scattering[4-7]. In electrical engineering, a waveguide couples two electromagnetic waves to produce parametric oscillators and parametric amplifiers[8]. A laser can be thought of as a coupled mode system, two of the modes being the population densities of the higher energy level and the lower energy level, the third mode being the population density of photons[9]. In plasma physics, an electromagnetic wave in an isotropic plasma can decay into: an electron wave and an ion-accoustic wave, the parametric decay instability[10-14]; two electron waves, the $2\omega_p$ or Goldman-Jackson[15,16] instability; an electron wave and another electromagnetic wave, called Raman scattering[17-19]; an ion-acoustic wave and an electromagnetic wave, called Brillouin scattering[18,20-22]. An electromagnetic wave in an anisotropic plasma has additional three-wave interactions[23-25].

Each of these interactions can be described by a system of three equations, each one a partial differential equation in space and time governing the evolution of one of the modes, including the effects due to the other two modes. There are then two alternatives: (a) Solve all three equations on the same footing. This has been done by many workers[26-33]; we will not be concerned with this procedure here. (b) Assume that one wave, called the pump, is much larger than the two others, and that over times of interest its magnitude does not change

appreciably. Then we can discard the equation for its evolution, and we are left with two linear coupled mode equations. The amplitude of the pump appears as a parameter in these two equations. It is th' procedure which will be followed here.

The standard coupled mode equations, in one dimension, for the amplitudes of the waves of interest are

$$\begin{aligned}(\partial_t + \nu_1 + V_1\partial_x)\, a_1(x,t) &= \gamma_o\, a_2(x,t) \\ (\partial_t + \nu_2 + V_2\partial_x)\, a_2(x,t) &= \gamma_o\, a_1(x,t)\end{aligned} \tag{1}$$

where V_1 and V_2 are the group velocities of waves 1 and 2, having either sign; ν_1 and ν_2 are the damping rates of waves 1 and 2 in the absence of coupling; γ_o (real and positive) represents the coupling of the two waves due to the presence of the pump wave, assumed constant over times of interest; $a_1(x,t)$ and $a_2(x,t)$ are the slowly varying amplitudes of waves 1 and 2; i.e., $\partial_t\left[\ln a_1(x,t)\right] \ll \omega_1$, $\partial_x\left[\ln a_1(x,t)\right] \ll k_1$, where (ω_1,k_1) are the frequency and wave number of wave 1; and likewise for wave 2.

Given suitable initial conditions and boundary conditions, Eqs. (1) can be solved. Before doing so, we give two examples of the derivation of Eqs. (1) from first principles.

First, suppose we have two normal mode oscillations in a medium, in the absence of the third wave, described by the following wave equations:

$$\begin{aligned}(\partial_t^2 - 2i\nu_1\partial_t + a_1^2 - v_1^2\partial_x^2)\,\phi_1(x,t) &= 0 \\ (\partial_t^2 - 2i\nu_2\partial_t + a_2^2 - v_2^2\partial_x^2)\,\phi_2(x,t) &= 0\ .\end{aligned} \tag{2}$$

Assuming solutions of the form $\phi_j(x,t) \sim \exp(-i\omega_j t + ik_j x)$, $j = 1,2$, we obtain the normal mode frequencies

$$\omega_j^2 = a_j^2 + v_j^2 k_j^2 \qquad j = 1,2 \qquad (3)$$

where we have neglected ν_1, ν_2 as small. As examples, consider: electromagnetic waves, with $a_j = \omega_p$, $v_j = c$; Langmuir waves, with $a_j = \omega_p$, $v_j = 3^{\frac{1}{2}} v_e$; and ion acoustic waves, with $a_j = 0$, $v_j = c_s$ (sound speed).

In the presence of the third wave, Eqs. (2) are coupled together as follows[34] (In Raman scattering, EM → EM + Langmuir, these equations are obtained from Maxwell's equations plus the Lorentz force equation):

$$(\partial_t^2 - 2i\nu_1\partial_t + a_1^2 - v_1^2\partial_x^2)\,\phi_1(x,t) = \beta_1\,\phi_o(x,t)\,\phi_2^*(x,t)$$
$$(\partial_t^2 + 2i\nu_1\partial_t + a_2^2 - v_2^2\partial_x^2)\,\phi_2^*(x,t) = \beta_2\,\phi_o^*(x,t)\,\phi_1(x,t) \qquad (4)$$

where β_1, β_2 are real coupling constants, $\phi_o(x,t)$ is the third (pump) wave, and we have taken the complex conjugate of the second equation. We now assume that each field quantity $\phi_j(x,t)$ can be written as a slowly varying (in space and time) amplitude times a rapidly varying (in space and time) phase: $\phi_j(x,t) = \tilde{\phi}_j(x,t) \exp(-i\omega_j t + ik_j x)$, $j = 0,1,2$. We further require the three-wave matching conditions: $\omega_o = \omega_1 + \omega_2$, $k_o = k_1 + k_2$. With these assumptions, and discarding terms in $\partial_x^2 a_j$, $\partial_t^2 a_j$, $j = 1,2$, Eqs. (4) become

$$\left[2i\omega_1\partial_t + 2i\nu_1\omega_1 + 2iv_1^2k_1\partial_x\right]\tilde{a}_1(x,t) = \beta_1\,\tilde{a}_o(x,t)\,\tilde{a}_2^*(x,t)$$

$$\left[-2i\omega_2\partial_t - 2i\nu_2\omega_2 - 2_1v_2^2k_2\partial_x\right]\tilde{a}_2^*(x,t) = \beta_2^*\,\tilde{a}_o^*(x,t)\,\tilde{a}_1(x,t)\ . \tag{5}$$

From Eq.(3), we obtain the group velocities $V_j \equiv \partial\omega_j/\partial k_j = v_j^2k_j/\omega_j$, and defining $\gamma_o \equiv (\beta_1\beta_2/4\omega_1\omega_2)^{\frac{1}{2}}\,\tilde{a}_o(x,t)$ we have

$$\left[\partial_t + \nu_1 + V_1\partial_x\right]\tilde{a}_1(x,t) = -i\sqrt{\frac{\beta_1\omega_2}{\beta_2\omega_1}}\,\gamma_o(x,t)\,\tilde{a}_2^*(x,t)$$

$$\left[\partial_t + \nu_2 + V_2\partial_x\right]\tilde{a}_2(x,t) = i\sqrt{\frac{\beta_2\omega_1}{\beta_1\omega_2}}\,\gamma_o^*(x,t)\,\tilde{a}_1(x,t)\ . \tag{6}$$

Defining $a_1(x,t) \equiv \tilde{a}_1(x,t)$; $a_2(x,t) \equiv -i(\beta_1\omega_2/\beta_2\omega_1)^{\frac{1}{2}}\,\tilde{a}_2^*(x,t)$ we find

$$\left[\partial_t + \nu_1 + V_1\partial_x\right]a_1(x,t) = \gamma_o\,a_2(x,t)$$

$$\left[\partial_t + \nu_2 + V_2\partial_x\right]a_2(x,t) = \gamma_o\,a_1(x,t)\ . \tag{7}$$

When γ_o is real and constant in space and time, these are just Eqs.(1).

In the presence of plasma <u>spatial</u> inhomogeneity, the derivation of Eqs. (1) must be modified. The inhomogeneity enters into Eqs.(4) through the parameters $\beta_1(x)$, $\beta_2(x)$, $\nu_1(x)$, $\nu_2(x)$, $\omega_p(x)$, $v_1(x)$, and $v_2(x)$. Each field quantity is now assumed to vary in a WKBJ sense as $\phi_j(x,t) = a_j(x,t)\exp\left[-i\omega_j t + i\int_{x_o}^{x} k_j(x')\,dx'\right]$, $j = 0,1,2$. That is, we choose $\{\omega_j\}$, and find $\{k_j(x)\}$ from the dispersion relation Eq. (3).

The frequencies are required to match, $\omega_o = \omega_1 + \omega_2$; we choose x_o to be the position where the wavenumber mismatch $\kappa(x)$ vanishes: $\kappa(x) \equiv k_o(x) - k_1(x) - k_2(x)$, $\kappa(x = x_o) = 0$. The derivation of Eqs.(5) remains unchanged, except that now we do not have $\exp i(k_o - k_1 - k_2)x = 1$, but rather $\exp i\int_{x_o}^{x} \left[k_o(x') - k_1(x') - k_2(x')\right] dx' \equiv \exp i\int_{x_o}^{x} \kappa(x')\, dx'$. The other steps remain unchanged, and Eqs.(1) are replaced by

$$\left[\partial_t + \nu_1 + V_1\partial_x\right] a_1(x,t) = \gamma_o(x)\, a_2(x,t) \exp\left[i\int_{x_o}^{x} \kappa(x')\, dx'\right] \tag{8}$$

$$\left[\partial_t + \nu_2 + V_2\partial_x\right] a_2(x,t) = \gamma_o(x)\, a_1(x,t) \exp\left[-i\int_{x_o}^{x} \kappa(x')\, dx'\right]$$

These equations were first introduced by Harker and Crawford[35], and much of the work on parametric instabilities in inhomogeneous plasma[34-75] is based on these equations. Despite the large amount of work on these equations in the years 1971-1975, new results are forthcoming, and much remains to be done. As evidence, of some sixty papers delivered at the Fifth Annual Anomalous Absorbtion Conference[76], held in Los Angeles in April, 1975, three papers were devoted entirely to solving these equations under various circumstances.

We present now an alternative derivation[77] of Eqs.(1), more general than the one above. Consider the model field equations

$$D_1(i\partial_t, -i\partial_x)\,\phi_1 = \Gamma\,\phi_o\,\phi_2^* \qquad (9)$$

$$D_2(i\partial_t, -i\partial_x)\,\phi_2 = \Gamma\,\phi_o\,\phi_1^*$$

where D_1 and D_2 are linear differential operators acting on the wave amplitudes ϕ_1, ϕ_2; ϕ_1 and ϕ_2 are coupled to the third wave ϕ_o through the coupling constant Γ. Assuming that each wave varies as

$$\phi_j(x,t) = \tilde{\phi}_j(x,t)\, e^{-i\omega_j t + ik_j x} \qquad (10)$$

where ω_1 and ω_2 are chosen to satisfy $\omega_o = \omega_1 + \omega_2$; k_j is obtained from ω_j through the equation $\mathrm{Re}\left[D_j(\omega_j, k_j)\right] = 0$, $j = 1,2$; and again $k_o = k_1 + k_2$. (In general, of course, all of these equalities may not be self consistent; we assume here that they are.) Equations (9) become

$$D_1(\omega_1 + i\partial_t, k_1 - i\partial_x)\,\tilde{\phi}_1 = \Gamma\,\tilde{\phi}_o\,\tilde{\phi}_2^* \qquad (11)$$

$$D_2(\omega_2 + i\partial_t, k_2 - i\partial_x)\,\tilde{\phi}_2 = \Gamma\,\tilde{\phi}_o\,\tilde{\phi}_1^* \ .$$

Taylor expanding the operators D_1, D_2 about (ω_1, k_1), (ω_2, k_2), we find

$$\left\{ \mathrm{Re}\left[D_1(\omega_1,k_1)\right] + i\,\mathrm{Im}\left[D_1(\omega_1,k_1)\right] + \left.\frac{\partial D_1}{\partial \omega}\right|_{\omega_1,k_1} i\,\partial_t - \left.\frac{\partial D_1}{\partial k}\right|_{\omega_1,k_1} i\partial_x \right\} \tilde{\phi}_1$$

$$= \Gamma\,\tilde{\phi}_o\,\tilde{\phi}_2^*$$

Equation (12) continued next page

Equation (12) continued

$$\left\{ \mathrm{Re}\left[D_2(\omega_2,k_2)\right] + i\,\mathrm{Im}\left[D_2(\omega_2,k_2)\right] + \left.\frac{\partial D_2}{\partial\omega}\right|_{\omega_2,k_2} i\,\partial_t - \left.\frac{\partial D_2}{\partial k}\right|_{\omega_2,k_2} i\,\partial_x \right\} \tilde{\phi}_2 = \Gamma\,\tilde{\phi}_o\,\tilde{\phi}_1^{*} \quad .$$

Dividing out the coefficient of ∂_t in each equation; recalling that $\mathrm{Re}\left[D_j(\omega_j,k_j)\right] = 0$, $j = 1,2$; introducing the damping rates

$$\nu_j \equiv \frac{\mathrm{Im}\left[D_j(\omega_j,k_j)\right]}{\left.\frac{\partial D_j}{\partial\omega}\right|_{\omega_j,k_j}} ; \qquad j = 1,2 ; \tag{13}$$

we have from Eq. (12)

$$\left[\partial_t + \nu_1 + V_1\partial_x\right]\tilde{\phi}_1 = \frac{\Gamma\,\tilde{\phi}_o}{i\left.\frac{\partial D_1}{\partial\omega}\right|_{\omega}}\,\tilde{\phi}_2^{*}$$

(14)

$$\left[\partial_t + \nu_2 + V_2\partial_x\right]\tilde{\phi}_2^{*} = \frac{\Gamma\,\tilde{\phi}_o^{*}}{-i\left.\frac{\partial D_2}{\partial\omega}\right|_{\omega_2,k_2}}\,\tilde{\phi}_1 \quad .$$

Define $\gamma_o^{\,2} \equiv \dfrac{\Gamma^2|\tilde{\phi}_o|^2}{\left.\frac{\partial D_1}{\partial\omega}\right|_{\omega_1,k_1}\left.\frac{\partial D_2}{\partial\omega}\right|_{\omega_2,k_2}}$; $a_1 \equiv \tilde{\phi}_1$; $a_2 \equiv \dfrac{-i\,\tilde{\phi}_2^{*}}{\left(\left.\frac{\partial D_1}{\partial\omega}\right|_{\omega_1,k_1}\left.\frac{\partial D_2}{\partial\omega}\right|_{\omega_2,k_2}\right)^{\frac{1}{2}}}$;

then we find, assuming γ_o real and positive,

$$(\partial_t + \nu_1 + V_1\partial_x)\, a_1(x,t) = \gamma_o\, a_2(x,t)$$

$$(\partial_t + \nu_2 + V_2\partial_x)\, a_2(x,t) = \gamma_o\, a_1(x,t) \qquad (15)$$

which are just Eqs. (1).

These have been two different derivations of Eqs. (1). The rest of this report is devoted to the solution of Eqs.(1), and their inhomogeneous counterpart Eqs.(8), in various situations. We will find that different forms of the wavenumber mismatch $\kappa(x)$ give very different results for the evolution of a pulse, the main distinction being between absolute instabilities, which grow in time at fixed position for $t \to \infty$, and convective instabilities, which are bounded in time at fixed position.

B. Parametric Instabilities in Homogeneous Plasma

In this section, we discuss solutions of Eqs. (1), the coupled mode equations in a homogeneous medium. In subsection 1, the pump extends over infinite distance, $-\infty < x < \infty$, and we consider the stability properties for various initial conditions. In subsection 2, the pump is finite in extent, $0 \le x \le L$, and the stability properties are found to depend on the length L.

1. Pump Infinite in Extent

In this subsection, the pump extends from $x = -\infty$ to $x = \infty$. We first consider the response to a spatially uniform excitation. Next, we use Bers-Briggs analysis[78] to distinguish absolute and convective instabilities for the Green's function response. Finally, we discuss the exact Green's function.

We treat the temporal response of the system to a uniform excitation as follows. Ignoring spatial derivatives in Eqs. (1), we look for a solution $\sim \exp(-i\omega t)$, and find

$$\omega = -i\left(\frac{\nu_1 + \nu_2}{2}\right) \pm i\sqrt{\gamma_o^2 + \left(\frac{\nu_1 - \nu_2}{2}\right)^2} \quad . \tag{16}$$

(Note that this ω is a frequency associated with the slowly varying amplitudes $a_1(x,t)$, $a_2(x,t)$, and has nothing to do with the original frequencies of the three coupled modes.) For $\nu_1 = \nu_2 = 0$, Eq.(16) yields $\omega = \pm i\gamma_o$. For $\nu_1, \nu_2 \neq 0$ instability results when

$$\gamma_o > (\nu_1\nu_2)^{\frac{1}{2}} \equiv \gamma_c \quad . \tag{17}$$

In other words, there is instability when the pump strength exceeds a threshold determined by the geometric mean of the damping rates.

Next, we treat the temporal response to an excitation at $x = 0$: initial conditions $a_1(x,t=0) = \delta(x)$, $a_2(x,t=0) = 0$; boundary conditions $a_1(x = \pm\infty,t) = 0$, $a_2(x = \pm\infty,t) = 0$. As in Fried, Schmidt, and Gould[79], we perform a Bers-Briggs analysis on Eq. (8); with solution $\sim \exp(-i\omega t + ikx)$ we have the dispersion relation

$$(\omega + i\nu_1 - kV_1)(\omega \quad i\nu_2 - kV_2) + \gamma_o^2 = 0 \quad . \tag{18}$$

For $V_1V_2 > 0$ there is only convective instability, with convective growth rate* given by Eq.(18) with $k = 0$; thus the threshold is the same as in Eq. (17) of the last paragraph, or

(19)

---

* The convective growth rate is that measured by an observer moving with the pulse peak. The absolute growth rate is that measured at fixed position.

$$\gamma_o > \gamma_c \quad . \tag{19}$$

For $V_1V_2 < 0$, Eq.(19) again determines the threshold for convective instability, but there is absolute instability at a higher threshold:

$$\gamma_o > \gamma_a \equiv \frac{\nu_1|V_2| + \nu_2|V_1|}{2\sqrt{V_1V_2}} \quad . \tag{20}$$

In terms of the basic length $L_o \equiv |V_1V_2|^{\frac{1}{2}}/\gamma_o$, and the spatial damping rates $\kappa_1 \equiv \nu_1/|V_1|$, $\kappa_2 \equiv \nu_2/|V_2|$, criterion (20) states

$$L_o^{-1} > \tfrac{1}{2}(\kappa_1 + \kappa_2) \tag{21}$$

which says that the spatial growth rate must exceed the arithmetic mean spatial damping rate in order for absolute instability to occur. The growth rate γ of the absolute instability, with $\nu_1 = \nu_2 = 0$, is

$$\gamma = 2\gamma_o \frac{|V_1V_2|^{\frac{1}{2}}}{|V_1| + |V_2|} \quad . \tag{22}$$

If $|V_1| = |V_2|$, we have the absolute growth rate $\gamma = \gamma_o$, which is the same growth rate obtained above for the uniform excitation in the absence of damping. The reason is that when $V_2 = -V_1$, the peak of the pulse remains at $x = 0$; the absolute and convective growth rates are then equal and are obtained from the dispersion relation (18) with $k = 0$.

Exact solutions to Eqs. (1) (the Green's functions) giving the response of the system to the initial conditions (23), $a_1(x,t = 0) = \delta(x)$, $a_2(x,t = 0) = 0$, can be obtained in a straightforward fashion by Laplace transforming in time $(t \to \omega)$ and Fourier transforming in space $(x \to k)$. The responses $a_1(x,t)$ and $a_2(x,t)$

are then obtained as an inverse Fourier-Laplace transform. Cassedy and Evans[80] first perform the inverse Laplace transform, and then the inverse Fourier transform, for $V_1V_2 > 0$ and for $V_1V_2 < 0$. Bobroff and Haus[81] perform the inverse Fourier transform first, and then the inverse Laplace transform, for the case $V_1V_2 < 0$. Kroll[7] and Kelley[82] have also treated this problem. We note that the sign of V_1V_2 depends on the observer's frame of reference; in particular, it is always possible to transform to a frame where $V_2 = -V_1$; thus we need only do this case.

The number of independent parameters in Eqs. (1) can be made explicit by defining the dimensionless variables:

$$T \equiv \gamma_o t; \quad L_o \equiv \frac{\sqrt{|V_1V_2|}}{\gamma_o}; \quad X \equiv \frac{x}{L_o}; \tag{24}$$

$$D_1 \equiv \nu_1/\gamma_o; \quad D_2 \equiv \nu_2/\gamma_o; \quad \beta \equiv \left|\frac{V_2}{V_1}\right| .$$

Substituting these new variables into Eqs.(1), we find

$$\left[\partial_T + D_1 + \frac{1}{\sqrt{\beta}}\partial_X\right] a_1(X,T) = a_2(X,T)$$

$$\left[\partial_T + D_2 \pm \sqrt{\beta}\,\partial_X\right] a_2(X,T) = a_1(X,T) \tag{25}$$

where the top sign is for $V_2 > 0$, the bottom sign is for $V_2 < 0$, and we always take $V_1 > 0$.

In the form Eq. (25), the coupled mode equations have only three independent parameters: D_1, D_2, β.

An example of the solution of Eqs.(25), with the initial conditions (23), is shown in Fig. 1, taken from Bobroff and Haus[81]. Here we see the temporal-spatial evolution of $a_1(X,T)$, $a_2(X,T)$, for $D_1 = 0$, $D_2 = 0$, $V_2/V_1 = -1$ ($\beta = 1$). This is an example of an absolute instability, where $a_1(X = 0,T)$, $a_2(X = 0,T)$ grow for all time.

Equations (25) may be further simplified by the substitution[81]

$$a_J(X,T) \equiv A_J(X,T) \exp\left[\left(-D_1 + \frac{D_1 - D_2}{1 \mp \beta}\right)T - \sqrt{\beta}\left(\frac{D_1 - D_2}{1 \mp \beta}\right)X\right] ; \quad J = 1,2 . \tag{26}$$

Then Eqs. (25) become

$$\left(\partial_T + \frac{1}{\sqrt{\beta}}\,\partial_X\right) A_1(X,T) = A_2(X,T)$$
$$\left(\partial_T \mp \sqrt{\beta}\,\partial_X\right) A_2(X,T) = A_1(X,T) . \tag{27}$$

The effects of damping have now been formally removed, and the only remaining explicit parameter is V_2/V_1 (β plus a sign). If we now make a Galilean transformation to a frame where $\beta = 1$ ($V_2 = -V_1$), we have no remaining parameters:

$$\left(\partial_T + \partial_X\right) A_1 = A_2$$
$$\left(\partial_T - \partial_X\right) A_2 = A_1 . \tag{28}$$

Eliminating A_2, we find

$$\left(\partial_T^2 - \partial_X^2 - 1\right) A_1(X,T) = 0 \tag{29}$$

which would be the well-known Klein-Gordon equation[83] if the sign of -1 were reversed. The Green's function of (29) is a modified Bessel function, yielding the behavior shown in Fig. 1.

2. Pump Finite in Extent

We next consider the case where the pump, represented by γ_o, exists over only the finite range $0 \le x \le L$ (see Fig. 2). We can regard this either as the case of Eqs. (1) with boundary conditions at $x = 0$, $x = L$; or as a special case of an inhomogeneous pump, with amplitude $\gamma_o = 0$ for $-\infty < x < 0$, $L < x < +\infty$: and γ_o finite for $0 \le x \le L$. The usual boundary conditions specify that a right going ($V_j > 0$) amplitude $a_j(x,t)$ vanish at the left boundary, $a_j(x = 0,t) = 0$; and that a left going ($V_j < 0$) amplitude vanish at the right boundary, $a_j(x = L,t) = 0$.

The most important question we may ask is this: Given an initial perturbation, is the time-asymptotic ($t \to \infty$) response bounded, or does it grow without bound? One way to answer this question is to look for normal modes in time; that is, a response which may depend on x but which has the time dependence $\exp(\gamma t)$: $a_j(X,T) \equiv a_j(X) \exp(\gamma T)$. Implicit in the work of Bobroff and Haus[81], this was carried out explicitly by Pesme, Laval, and Pellat[56]. Set $D_1 = D_2 = 0$ in Eqs. (25), and assume temporal dependence $\exp(\gamma T)$; then Eqs. (25) become

$$\left(\gamma + \frac{1}{\sqrt{\beta}}\,\partial_X\right) a_1(X) = a_2(X)$$

$$\left(\gamma \pm \sqrt{\beta}\,\partial_X\right) a_2(X) = a_1(X) \qquad (30)$$

For $V_1V_2 > 0$ the boundary conditions are $a_1(X = 0) = a_2(X = 0) = 0$. Finding no solution with $\gamma > 0$ for these boundary conditions, we conclude that no absolute instability exists for $V_1V_2 > 0$.

For $V_1V_2 < 0$ the boundary conditions are $a_1(X = 0) = a_2(X = L/L_o) = 0$. (We always take $V_1 > 0$, so here $V_2 < 0$.) Solving Eqs. (30) with these boundary conditions, we find unstable normal modes when

$$L > \frac{\pi}{2} L_o \quad . \tag{31}$$

We can understand this threshold heuristically as follows. Consider Eqs. (1) with $V_1 = -V_2 \equiv V$, and suppose that $|a_1(x,t)|^2$ represents an energy density. Suppose further that $a_1(x,t)$ and $a_2(x,t)$ are equal and independent of x. Then from Eqs. (1) with $\nu_1 = \nu_2 = 0$, $\partial_t a_1 = \gamma_o a_2 \sim \gamma_o a_1$. Multiply by a_1; then ignoring factors of 2 we find $\partial_t |a_1|^2 \sim \gamma_o |a_1|^2$. The time rate of increase of energy in the system is then $\partial_t \left[L|a_1|^2 \right] \sim \gamma_o L|a_1|^2$. The rate of loss of energy through the sides is $\sim V|a_1|^2$. For net energy gain, we need (rate of energy increase) > (rate of energy loss), or $\gamma_o L|a_1|^2 > V|a_1|^2$, or $L > V/\gamma_o = L_o$. The latter corresponds to Eq. (29).

The temporal growth rate itself is given by the formula

$$\gamma = \frac{\sqrt{\beta}}{1 + \beta} \eta \tag{32}$$

where

$$\eta = \mp 2\cos y \tag{33}$$

and y is a solution of

$$\frac{\sin y}{y} = \pm \frac{L_o}{L} \quad . \tag{34}$$

The top (bottom) signs in Eqs. (33) and (34) go together. (See Fig. 3.) For $0 \le L/L_o \le 1$ there is no real solution to Eq. (32). For $1 \le L/L_o < \pi/2$, there is a solution y for the top sign in Eq. (34), giving $\eta < 0$ and so a stable solution $\gamma < 0$. For $(n + \frac{1}{2})\pi \le L/L_o \le (n + \frac{3}{2})\pi$, $n = 1,2,3,\cdots$, there are $2n+1$ roots to Eq.(34), roughly half of which correspond to unstable γ's. The most unstable mode is always the one at the smallest value of y. Figure 3, adapted from Bobroff and Haus[81], shows the graphical solution of Eq.(34) for $L/L_o = (9/2)\pi$; there are four stable roots and five unstable roots.

For very large L/L_o, $y \approx \pi$, $\eta \approx +2$, and $\gamma \approx 2\beta^{\frac{1}{2}}/(1 + \beta)$ In dimensional units, this is

$$\gamma \approx 2\gamma_o \frac{\sqrt{|V_1 V_2|}}{V_1 + |V_2|} \tag{35}$$

which is the same as Eq.(22) for the medium of infinite extent.

There is an alternative derivation of the threshold Eq. (31), due to Liu and Nishikawa[84], which uses the well-known properties of the Schrödinger equation. Consider Eqs. (1) with $\nu_1 = \nu_2 = 0$, and eliminate $a_2(x,t)$; we have

$$(\partial_t + V_2\partial_x)(\partial_t + V_1\partial_x)\, a_1(x,t) - \gamma_o^2\, a_1(x,t) = 0 \quad . \tag{36}$$

Laplace transform in time, neglect initial conditions, and divide by V_1V_2; then

$$\left[\partial_x^2 + \left(\frac{\gamma}{V_1} + \frac{\gamma}{V_2}\right)\partial_x + \frac{\gamma^2 - \gamma_o^2}{V_1 V_2}\right] a_1(x,t) = 0 \quad . \tag{37}$$

Define

$$\psi(x,t) \equiv a_1(x,t) \exp\left[\frac{1}{2}\left(\frac{\gamma}{V_1} + \frac{\gamma}{V_2}\right)x\right] \tag{38}$$

and find

$$-\partial_x^2 \psi \pm L_o^{-2}\psi = -\frac{1}{4}\left(\frac{\gamma}{V_1} - \frac{\gamma}{V_2}\right)^2 \psi. \tag{39}$$

This is just Schrodinger's equation for a square well potential: $L_o^{-2} \equiv \gamma_o^2/|V_1 V_2|$ is finite, $0 \le x \le L$, and zero otherwise. If we can find an unstable eigenvalue $Re(\gamma) > 0$, with eigenfunction $\psi_\gamma(x)$ corresponding to a bound state, then we have an absolute instability. For $V_1 V_2 > 0$ (top sign in Eq. (39)), there is a potential hump, and thus no bound state. For $V_1 V_2 < 0$ (bottom sign in Eq. (39)), there is a potential well. Apply the boundary conditions $\psi(x = \pm\infty) = 0$, and assume the solution

$$\psi(x) = \begin{cases} \exp(+k_o x) & -\infty < x < 0 \\ A e^{ikx} + B e^{-ikx} & 0 \le x \le L \\ \exp(-k_o x) & L < x < \infty \end{cases} \tag{40}$$

where $k_o = \frac{\gamma}{2}\left(\frac{V_1 - V_2}{V_1 V_2}\right)$, $k = \sqrt{L_o^{-2} - k_o^2}$, $V_1 > 0$, $V_2 < 0$. Requiring the continuity of ψ and $\frac{\partial \psi}{\partial x}$ at $x = 0$ and $x = L$, we find an eigenvalue condition which is equivalent to Eq.(31).

In a somewhat different approach, Kroll and Kelley[82] considered the temporal evolution of a pulse in a finite, homogeneous medium, with the further specification that the pump be square in time

and in space. They found different qualitative behaviors in three temporal regimes: short, intermediate, and long.

Gorbunov[85] considered the case $V_2 = 0$, where we know there are no temporally growing solutions. Assuming $V_1 < 0$, he applies a constant level $a_1(x = L,t) = C_1$ at the boundary. With initial conditions $a_1(x,t = 0) = C_1$, $a_2(x,t = 0) = C_2$, he finds that the transient response at early times can be orders of magnitude greater than the final steady state response. We have verified this result by direct numerical integration of the equations.

There are several analytic methods for obtaining exact Green's functions for the finite, homogeneous system. The results of one of these, taken from Bobroff and Haus[81], are shown in Fig. 4, for an absolutely unstable case. A particularly interesting method, based on the concept of "reflections", is discussed in Appendix A.

C. The Effects of Inhomogeneity

So far we have discussed only a homogeneous medium in the presence of a homogeneous pump, of finite or infinite extent, represented by γ_0. We now wish to discuss the possibility that the pump and the medium are inhomogeneous. Pump inhomogeneity can be introduced by simply allowing

$$\gamma_0 = \gamma_0(x) \quad . \tag{41}$$

Inhomogeneity of the medium is introduced through the wave number mismatch $\tilde{\kappa}(x)$, as discussed in Section I-A. With both types of inhomogeneity, Eqs. (8) become

$$\left[\partial_t + \nu_1 + V_1\partial_x\right] a_1(x,t) = \gamma_o(x) \exp\left[i \int_{x_o}^{x} \bar{\kappa}(x')\, dx'\right] a_2(x,t) \tag{42}$$

$$\left[\partial_t + \nu_2 + V_2\partial_x\right] a_2(x,t) = \gamma_o(x) \exp\left[-i \int_{x_o}^{x} \bar{\kappa}(x')\, dx'\right] a_1(x,t)$$

where we again assume $\gamma_o(x)$ real. Taylor expanding the function $\bar{\kappa}(x)$ about the point $x_o = 0$, and keeping only the first term $x\, d_x\, \bar{\kappa}(x)\Big|_{x=0} \equiv \bar{\kappa}' x$, we have

$$(\partial_t + \nu_1 + V_1\partial_x)\, a_1(x,t) = \gamma_o(x) \exp\left[i\bar{\kappa}'\, x^2/2\right] a_2(x,t) \tag{43}$$

$$(\partial_t + \nu_2 + V_2\partial_x)\, a_2(x,t) = \gamma_o(x) \exp\left[-i\bar{\kappa}'\, x^2/2\right] a_1(x,t) \quad .$$

Ignoring ν_1 and ν_2, which could be removed by the transformation Eq. (26), we define dimensionless variables

$$\begin{aligned} T &\equiv \gamma_o(x = 0)t \\ L_o &\equiv |V_1 V_2|^{\frac{1}{2}}/\gamma_o(x = 0) \\ X &\equiv x/L_o \\ \beta &\equiv |V_2/V_1| \\ \kappa' &\equiv \bar{\kappa}'\, L_o^{\,2} \\ \lambda &= 1/\kappa' = \gamma_o^{\,2}/\bar{\kappa}'|V_1 V_2| \end{aligned} \tag{44}$$

and obtain from Eqs. (43)

$$\left(\partial_T + \frac{1}{\sqrt{\beta}}\,\partial_X\right) a_1(X,T) \;=\; \frac{\gamma_o(X)}{\gamma_o(0)} \exp\left[i\kappa' X^2/2\right]\, a_2(X,T)$$

$$\left(\partial_T \pm \sqrt{\beta}\,\partial_X\right) a_2(X,T) \;=\; \frac{\gamma_o(X)}{\gamma_o(0)} \exp\left[-i\kappa' X^2/2\right]\, a_1(X,T) \quad . \tag{45}$$

Note that inhomogeneity of the pump enters as a real amplitude of X; inhomogeneity of the plasma as a complex function of X, with unit absolute value; we might therefore suspect that the effects of these two types of inhomogeneities are entirely different.

1. Inhomogeneous Plasma, Homogeneous Pump

In this section, we consider Eqs. (45) in their dimensionless form, with $\kappa(X) \equiv L_o \bar{\kappa}(x)$, and with $\gamma_o(x)$ = constant, $-\infty < x < \infty$; then

$$\left(\partial_T + \frac{1}{\sqrt{\beta}}\,\partial_X\right) a_1(X,T) \;=\; a_2(X,T) \exp\left[\, i \int_0^X \kappa(X')\, dX' \right]$$

$$\left(\partial_T \pm \sqrt{\beta}\,\partial_X\right) a_2(X,T) \;=\; a_1(X,T) \exp\left[-i \int_0^X \kappa(X')\, dX' \right] \quad . \tag{46}$$

We ask the following question: Given an initial perturbation

$$a_1(X, T=0) \;=\; 0 \;; \qquad a_2(X, T=0) \;=\; \delta(X) \tag{47}$$

are there any solutions $a_1(X,T)$ which remain unbounded as $T \to \infty$. This question was first answered by Piliya[58] for the case $V_1 V_2 > 0$, and then by Rosenbluth[57] for arbitrary $V_1 V_2$, both for the case $\kappa(X) = \kappa' X$. In an elegant application of WKBJ theory[86], Rosenbluth[57]

showed that for arbitrary V_1V_2, there is no absolute instability for $T \to \infty$, but rather a saturation of the amplitudes $|a_1(X,T)|$ and $|a_2(X,T)|$ at a value $\sim\exp(\pi\lambda)$ where $\lambda \equiv \kappa'^{-1}$. Note that this does not correspond to Briggs' usual definiton of convective instability[78] either, since the amplitude asymptotes to a certain level $\exp(\pi\lambda)$ (when $\nu_1 = \nu_2 = 0$) rather than falling to zero.

In the case $\kappa(X) = \frac{1}{2}\kappa'' X^2$, with κ'' = constant, Rosenbluth[57] showed that for $V_1V_2 < 0$ there can be an absolute instability for sufficiently large γ_0. In Appendix B we discuss these results in relation to the general criterion for absolute instabilities in an inhomogeneous medium proposed by Sudan[87].

The exact solution of Eqs. (46) with initial conditions (47), and with $\kappa(X) = \kappa' X$, was first worked out by Rosenbluth, White, and Liu[60]. Their exact results were in good agreement with the WKBJ results of Rosenbluth[57]. Figure 5 shows the evolution of $|a_1(X,T)|$ for the case $V_1V_2 < 0$, $\beta = -0.2$, $\kappa' = 1$, taken from Rosenbluth, White, and Liu[60]. Figure 6 shows the results of our direct numerical integration of Eqs. (46) for the same case. Figure 6 also shows the behavior of $|a_2(X,T)|$, which includes a pulse growing $\propto T$ following the initial delta-function. For $|a_1(X,T)|$ we see the same behavior as in the work of Rosenbluth, White, and Liu[60], (Fig. 5), except that the saturation occurs at a value somewhat less than $\exp(\pi\lambda)$. This is due to a factor which was dropped in the last half of Ref. 60; for $V_2 = -V_1$ this factor is $\left[2(2\pi)^{\frac{1}{2}}\right]^{-1}$. With its inclusion, our results are in exact agreement with Ref. 60.

An alternative solution to Eqs. (46), with $\kappa(X) = \kappa' X$, was provided by Laval, Pellat, and Pesme[61], and independently by Kaufman[62].

By making a transformation of variables, Eqs. (43) can be put in the form

$$\partial_T^2 b(T) - f(T)\, b(T) = 0 \quad . \tag{48}$$

In this form $\gamma \equiv \sqrt{f(T)}$ is found to be real and positive only for a finite time, implying no absolute instability. The form of $f(T)$ also provides easy access to the result $|a_1(X, T \to \infty)| \sim \exp(\pi\lambda)$.

We consider next the form $\kappa(X) = A \tanh(BX)$, which is a possible model of the junction between two regions of homogeneous plasma with different densities. By direct numerical integration of Eqs. (46) we obtain the behavior shown in Fig. 7, for $A = 10$, $B = \frac{1}{10}$, and $V_2/V_1 = -1$. With these parameters, $d\kappa/dX\big|_{X=0} = 1$, and the region of nearly constant $d\kappa/dX$ is large enough to see the beginning of convective saturation. The pulse response to the initial conditions $a_1(X, T = 0) = \delta(X)$, $a_2(X, T = 0) = 0$, grows initially with the homogeneous growth rate $\gamma = 1$ (see Eq. (22), which in dimensional units yields $\gamma/\gamma_o = 1$). The pulse begins to saturate at $\sim\exp(\pi\lambda)$, then feels the homogeneous regions and takes off again at the homogeneous growth rate $\gamma = 1$.

2. Homogeneous Plasma, Inhomogeneous Pump

We have already considered a special case of homogeneous plasma, inhomogeneous pump in Section I-B-2, where the pump was constant over the region $0 \leq x \leq L$, and zero otherwise. There we found an absolute instability only for $L/L_o > \pi/2$.

When the pump has a parabolic shape, and the medium is homogeneous, we have $\gamma_o(x) = \gamma_o(1 - x^2/L_\gamma^2)^{\frac{1}{2}}$ and $\bar{\kappa}(x) = 0$ in Eqs. (42). Following Liu and Nishikawa[84], we again put Eqs. (42) in the form of a Schrödinger equation. For $V_1 V_2 > 0$, we again find

a potential hump, no bound eigenfunctions, and no unstable eigenvalues. For $V_1V_2 > 0$, an infinite number of unsteble modes are found, with threshold pump width $L_\gamma/L_o = (2n + 1)$, $n = 0,1,2,\cdots$, for onset of the nth mode. With damping, and taking the limit $L_\gamma \to \infty$, the homogeneous medium threshold is regained (See Eq.(21)); when both the damping threshold and pump length threshold are greatly exceeded the modes grow at nearly the largest possible growth rate, $\gamma/\gamma_o \approx 1$. From the form of the eigenfunction solution to the Schrodinger equation, it can be seen that the absolutely growing modes are localized with characteristic dimension $\sim(L_\gamma L_o)^{\frac{1}{2}}$.

3. Inhomogeneous Plasma and Pump

We turn now to the study of Eqs. (42) in their full complexity:

$$\left(\partial_t + \nu_1 + V_1\partial_x\right) a_1(x,t) = \gamma_o(x)\, a_2(x,t) \exp\left[i\int_0^x \bar{\kappa}(x')\,dx'\right] \tag{49}$$

$$\left(\partial_t + \nu_2 + V_2\partial_x\right) a_2(x,t) = \gamma_o(x)\, a_1(x,t) \exp\left[-i\int_0^x \bar{\kappa}(x')\,dx'\right].$$

The simplest case, and the most enlightening, involves a pump existing over a finite region, γ_o = constant, $0 \le x \le L$, and zero otherwise; and a linear inhomogeneity of the plasma, $\bar{\kappa}(x) = \bar{\kappa}'x$. This configuration is sketched in Fig. 8. First considered by Forslund, Kindel, and Lindman[63], and by Pesme, Laval, and Pellat[56], additions to the theory of this case have been made by: the present author, to be discussed below; Jha and Srivastava[75]; Dubois, Forslund, and Williams[65]; and Chambers and Bers[66].

Recall first that when $\bar{\kappa}' = 0$, this is just the case considered in Section I-B-2, the finite pump, homogeneous plasma case.

There we found absolute instability for $L/L_o > \pi/2$; we expect that very small inhomogeneity κ' will not change this qualitative behavior.

Forslund, Kindel, and Lindman[63] proceed as follows. With $\tilde{\kappa}(x) = \tilde{\kappa}'x$, assume a solution $a_1(x,t) = a_1(x)\exp(\tilde{\gamma}t)$, $a_2(x,t) = a_2(x)\exp(\tilde{\gamma}t)$; then Eqs. (42) become

$$\left[\tilde{\gamma} + V_1\partial_x\right]a_1(x) = \gamma_o \tilde{a}_2(x)$$

$$\left[\tilde{\gamma} + V_2\partial_x - iV_2\,\tilde{\kappa}(x)\right]\tilde{a}_2(x) = \gamma_o\, a_1(x) \tag{50}$$

where $\tilde{a}_2(x) = a_2(x)\exp\left[i\int_o^x \tilde{\kappa}(x')\,dx'\right]$. Define a new space scale $\tilde{X} \equiv x\gamma_o/V_1$; then Eqs. (50) are

$$\left(\tilde{\gamma}/\gamma_o + \partial_{\tilde{X}}\right)a_1(\tilde{X}) = \tilde{a}_2(\tilde{X})$$

$$\left(\frac{\tilde{\gamma}V_1}{\gamma_o V_2} + \partial_{\tilde{X}} - i\kappa(\tilde{X})\right)\tilde{a}_2(\tilde{X}) = a_1(\tilde{X}) \tag{51}$$

where $\kappa(\tilde{X}) \equiv \tilde{\kappa}(x)\,V_1/\gamma_o$. Assume now that $|V_2/V_1| \ll 1$, and define a new temporal quantity $\gamma \equiv \frac{\tilde{\gamma}}{\gamma_o}\frac{V_1}{V_2}$; then Eqs.(49) are

$$\left(\gamma\, V_2/V_1 + \partial_{\tilde{X}}\right)a_1(\tilde{X}) = \tilde{a}_2(\tilde{X})$$

$$\left(\gamma + \partial_{\tilde{X}} - i\kappa(\tilde{X})\right)\tilde{a}_2(\tilde{X}) = a_1(\tilde{X}) \ . \tag{52}$$

Since $|V_2/V_1| \ll 1$ we can neglect the first term in the first equation, being left to solve

$$\partial_{\tilde{X}} \tilde{a}_1(\tilde{X}) = \tilde{a}_2(\tilde{X})$$

$$\left(\gamma + \partial_{\tilde{X}} - i\kappa(\tilde{X})\right)\tilde{a}_2(\tilde{X}) = a_1(\tilde{X}) \qquad (53)$$

with $\kappa(\tilde{X}) = \kappa'\tilde{X}$. We wish to find the eigenvalue γ. With $V_1 > 0$, $V_2 < 0$ we have the boundary conditions $a_1(\tilde{X} = 0) = 0$, $\tilde{a}_2(\tilde{X} = \tilde{L}) = 0$, where $\tilde{L} \equiv L\gamma_0/V_1$. We guess a value for γ, set $a_1(\tilde{X} = 0) = 0$ and $\tilde{a}_2(\tilde{X} = 0) = 1$, and integrate the Eqs. (53) numerically from $\tilde{X} = 0$ to $\tilde{X} = \tilde{L}$, where we desire $\tilde{a}_2(\tilde{X} = \tilde{L}) = 0$. Adjust the guessed value of γ until this is so; γ is then the desired eigenvalue. The results of this procedure are shown in Fig. 9, for the case $\tilde{L} = 5$, $V_1 = 24$, $V_2 = -1$, $\gamma_0 = \sqrt{24}$. For small κ', we find two real eigenvalues, in agreement with Section I-B-2 for the homogeneous ($\kappa' \to 0$) case. As κ' increases, the eigenvalues move together; at a particular value of κ' the two real roots merge to become two complex roots, complex conjugates. For very large κ', the real growth rate goes to zero and the instability disappears.

To verify these results, we have numerically integrated Eqs. (42). The large points in Fig. 9 are the eigenfrequencies obtained from our numerical integration; we see exact agreement with the results of Forslund, Kindel, and Lindman[63], within the accuracy of our numerical calculation.

We can gain further understanding of this problem by calculating the Green's function response of Eqs. (45) to the initial conditions

$$a_1(X, T = 0) = \delta(X) \quad , \qquad a_2(X, T = 0) = 0 \quad . \qquad (54)$$

Such a calculation, by direct integration of the fundamental equations, is shown in Fig. 10, where we plot $|a_1(X,T)|$ and $|a_2(X,T)|$ vs. X at different times T, for the parameters $\kappa' = 1$, $V_1 = 24$, $V_2 = -1$, $\gamma_o = \sqrt{24}$, $\bar{L} = 5$. (These parameters were chosen for easy comparison with Fig.9 and Fig. 11.) Here we see quite clearly the presence of two normal modes; in particular, at the point $X = 5$, we seem to have equal amounts of each normal mode, because at $T = 3.25$, $|a_1(X = 5, T = 32.5)| \approx 0$. We interpret this behavior as being of the form

$$|a_1(X = 5,T)| \sim |e^{(\gamma+i\Omega)T} + e^{(\gamma-i\Omega)T}| \sim e^{\gamma T}|e^{i\Omega T} + e^{-i\Omega T}|$$

$$\sim e^{\gamma T}|\cos(\Omega T)| \qquad (55)$$

which varies between a maximum value $\sim\exp(\gamma T)$ and a minimum value zero, just as seen in Fig. 10 at the position $X = 5$. This oscillating behavior, on top of the exponential growth, occurs in the time asymptotic response. This behavior differs from that of the finite, homogeneous case, seen in Fig. 4, where the asymptotic behavior consists of purely exponential growth at each position.

A further calculation by Forslund, Kindel, and Lindman[88] is shown in Fig. 11. Here we see the behavior of the fastest growing normal mode as a function of pump length $\bar{L}$, for fixed $\kappa' = 0.4$ ($V_1 = 24$, $V_2 = -1$, $\gamma_o = \sqrt{24}$, $\nu_1 = \nu_2 = 0$). The real part of the growth rate reaches a constant value for large pump length $\bar{L}$, while the imaginary part of the growth rate is linearly proportional to $\bar{L}$ for large $\bar{L}$.

At this point, we must pause to consider an apparent contradiction. Figure 11 predicts an absolute instability for fixed κ',

$\bar{L} \to \infty$, whereas the work of Rosenbluth[57], discussed in Section I-C-1, indicated no absolute instability.

There are two possible resolutions to this apparent contradiction. The first is that perhaps Rosenbluth[57] should have found a root $(\gamma + i\Omega)$ with finite growth rate γ and infinite imaginary part Ω, as indicated in Fig. 11 for $\bar{L} \to \infty$. It is possible that his WKBJ procedure could have missed such a root, since it would have an infinite absolute value.

The second possible resolution lies in the limiting procedures involved. Mathematically, Forslund[88] et al., take $T \to \infty$ first and then $L \to \infty$; Rosenbluth, on the other hand, takes $L \to \infty$ and then $T \to \infty$. It is well known mathematically that changing the order of limits can completely change the result; witness, for example, $\lim_{\substack{a\to 0 \\ b\to 0}} \frac{a}{a^2 + b^2}$, which yields either zero or infinity depending on the order of the limits. Physically, Forslund[88] et al. assume that each wave has had the chance to "reflect" many times from boundary to boundary, and vice versa. But Rosenbluth's[57] pulse never reaches the boundaries, and never has time to reflect. Thus, the absolute growth rate of Forslund[88] et al. never makes its appearance.

At this time, it is not clear whether one, or both, or neither, of the above resolutions is the appropriate one.

The Green's functions shown in Fig. 10 can be obtained analytically, as well as by direct numerical integration of the coupled mode equations. We have done this, and present the calculation in Appendix C. Due to the complexity of this solution, it is easier in practice to numerically integrate the basic equations.

Finally, let us briefly discuss three other contributions to this problem of finite pump, inhomogeneous plasma, Fig. 8. Jha and Srivastava[75] obtain an analytic solution for the growth rate $(\gamma + i\Omega)$, using perturbation theory for small κ'. Dubois, Forslund, and Williams[65] use the WKBJ theory to obtain approximate results for the growth rate $(\gamma + i\Omega)$ vs. pump length L and inhomogeneity κ'. They also considered the case $\gamma_0(x) \sim \sin^2(X/L_\gamma)$, $-L_\gamma < X < L_\gamma$, as well as other smooth functions for $\gamma_0(x)$. In all cases, results similar to those of this section were found. Chambers and Bers[66] solve Eqs. (42) in the same manner as we do in Appendix C. However, they look for a special value of temporal variable γ, rather than regarding γ as a Laplace transform variable to be integrated over. Applying boundary conditions at $X = 0$ and $X = L$, they find the eigenfrequency $\gamma + i\Omega$, which agrees exactly with those shown in Figs. 9 and 11. They next obtain the full spatial solution to Eqs. (42) in terms of parabolic cylinder functions. These solutions are found to hug the walls as $L \to \infty$, thus leaving no effect in the middle of the system. This phenomenon is claimed by Chambers and Bers[66] to provide yet a third possible resolution to the Forslund-Rosenbluth paradox.

Another interesting characteristic of the finite pump case is the following. With $V_1 > 0$, $V_2 < 0$, suppose the system is too short to be absolutely unstable. Then suppose we input a constant value $a_1(X = 0,T) = a_0$ at the left-hand boundary. What will be the amplification $a_1(X = L/L_0,T)a_0$, measured at the right-hand boundary after the steady state has been reached? For $V_2/V_1 = -1$, $L/L_0 = 1$, we determine the amplification A for various values of κ', by direct numerical integration. Figure 12 shows the results. We see

that the greatest amplification is for the homogeneous case $\kappa' = 0$, and the amplification decreases for increasing inhomogeneity.

We turn next to the work of White, Kaw, Pesme, Rosenbluth, Laval, Huff, and Varma[64], who considered the inhomogeneous pump, inhomogeneous medium case. Starting with the equations

$$(\partial_t + \nu_1 + V_1\partial_x)\, a_1(x,t) = \gamma_o(x)\, e^{i\int_0^x \bar{\kappa}(x')dx'}\, a_2(x,t) \tag{56}$$

$$(\partial_t + \nu_2 - V_2\partial_x)\, a_2(x,t) = \gamma_o(x)\, e^{-i\int_0^x \bar{\kappa}(x')dx'}\, a_1(x,t)$$

with $V_1, V_2 > 0$ (note the (-) sign in the second equation), $\gamma_o(x)$ is then expressed in the form

$$\gamma_o(x) = \gamma_o\, e^{\int_0^x \alpha(x')dx'} \quad . \tag{57}$$

Laplace transform in time, $f(p) \equiv \int_0^\infty e^{-pt} f(t)\, dt$, and define

$$a_2(x,p) = F(x,p) \exp\left[-\frac{1}{2}\left(\frac{p+\nu_1}{V_1} + \frac{p+\nu_2}{V_2}\right)x \right.$$

$$\left. + \frac{1}{2}\int_0^x \left[\alpha(x') + i\kappa(x')\right] dx' \right] \tag{58}$$

obtaining the equation for $F(x,p)$

$$d_x^{\,2} F(x,p) + f(x,p)\, F(x,p) = 0 \tag{59}$$

where

$$f(x,p) = -\frac{1}{4}\left[\alpha(x) - iK(x) - \left(\frac{p+\nu_1}{V_1} + \frac{p+\nu_2}{V_2}\right)\right]^2 +$$

$$+ \frac{1}{2}(\partial_x\alpha - i\partial_x\kappa) + \frac{\gamma_o^2}{V_1V_2}\, e^{2\int_0^x \alpha(x')dx'} \quad . \tag{60}$$

Choose a Gaussian profile for the pump, $\alpha(x) \equiv -2x/L_\gamma^2$, and let $\kappa(x) = \kappa' x$; we obtain

$$f(x) = -\left[x\left(\frac{1}{L_\gamma^2} + \frac{i\kappa'}{2}\right) + \frac{1}{2}\left(\frac{p+\nu_1}{V_1} + \frac{p+\nu_2}{V_2}\right)\right]^2$$

$$-\left(\frac{1}{L_\gamma^2} + \frac{i\kappa'}{2}\right) + \frac{\gamma_o^2}{V_1V_2}\, e^{-2x^2/L_\gamma^2} \quad . \tag{61}$$

From this point, White[64] et al. analyze Eq. (56) using WKBJ techniques[86] and looking for normal modes. For V_1 and V_2 in the same direction, there are no unstable normal modes. For V_1 and V_2 in opposite directions, there exists an unstable normal mode provided three necessary conditions for absolute instability are satisfied, namely

(i) the threshold for instability in an infinite, homogeneous medium must be satisfied, (see Eq. (21)) namely

$$\gamma_o > \frac{\nu_1|V_2| + \nu_2|V_1|}{2\sqrt{V_1V_2}} \quad ; \tag{62}$$

(ii) we require $L_\gamma > L_o$. This corresponds to the threshold for absolute instability in a homogeneous plasma with finite length pump, Section I-B-2. (See Eq. (29).)

(iii) we require

$$L_\gamma/L_o > (1 + \bar{\kappa}' L_\gamma^2) \quad . \tag{63}$$

If $\kappa' L_\gamma^2 \gg 1$, this becomes

$$L_\gamma < \frac{1}{\kappa' L_o} \quad . \tag{64}$$

This upper bound on L_γ, perhaps surprising, could have been predicted on the basis of Section I-B-2, the infinite pump, inhomogeneous medium case, where we found no absolute instability; there we had $L_\gamma \to \infty$.

White[64] et al. interpret this upper bound on L_γ as being a condition on the sharpness of the boundary $\gamma_o(x)$, a sufficient amount of sharpness being necessary to cause the "reflections" needed to produce absolute instability. This interpretation is along the same lines as the "reflections" of Bobroff and Haus[81] (Appendix A). Another way to discuss this phenomenon is to say that in the infinite, inhomogeneous case there are destructive interferences, originating at large x, which quench the absolute instability. Cutting off the pump at large x destroys the source of these destructive interferences, allowing the absolute instability to exist.

In this section, we have been concerned with inhomogeneities which vary monotonically. In the next section, we consider non-monotonic inhomogeneities in the form of spatial turbulence.

II. PARAMETRIC INSTABILITIES IN THE PRESENCE OF LONG WAVELENGTH TURBULENCE

A. General Results

In this section, we discuss the influence of irregular inhomogeneities on parametric instabilities. First, we review previous work. Then we discuss our own work[67] on long wavelength turbulence, in the presence of a linear density gradient, for anti-parallel group velocities.

There is a substantial body of work on parametric instabilities driven by a pump which has finite bandwidth[89-95], the bandwidth being thought of as a random phase $\phi(t)$ in the temporal behavior of the pump, which varies $\sim \exp\left[-i\omega_o t + \phi(t)\right]$. An important effect is found when the bandwidth is of order γ_o.

The earliest treatment of three wave interactions in the presence of spatial turbulence is due to Tamoikin and Fainshtein[96], who consider all three equations and find that the turbulence suppresses the usual relaxation oscillations. There has also been some work on all three waves in the presence of a random phase, by Wilhelmsson[28].

The case of spatial turbulence in a homogeneous plasma, using Eqs. (42) with $\kappa(x)$ a random function characterized by amplitude $\Delta \equiv \left\langle \left[\bar{\kappa}(x)\right]^2 \right\rangle^{\frac{1}{2}}$ and correlation length L_T, has been considered by Kaw, White, Pesme, Rosenbluth, Laval, Varma, and Huff[69] for the case of parallel group velocities. For $L_o\Delta^2 L_T \gg 1 \gg L_T/L_o$, they find an increase in the growth length from L_o (for $\Delta = 0$) to $(L_o\Delta^2 L_T)L_o$.

Kaw[69] et al. have also considered, for parallel group velocities, the case of a linear density gradient in the presence of spatial turbulence, $\bar{\kappa}(x) = \bar{\kappa}'x + \delta\kappa(x)$, where $\delta\kappa(x)$ is the turbulent

wavenumber mismatch with correlation length $L_T \ll L_o$. We know that in the absence of turbulence, a constant input at $x = 0$ saturates spatially at a level $\exp(\pi\lambda)$, where $\lambda \equiv \gamma_o^2/(\bar{\kappa}'|V_1 V_2|)$. In the presence of turbulence, Kaw[69] et al. find the same result, spatial saturation at $\exp(\pi\lambda)$, but with an increased growth length before saturation.

We wish to generalize the results of the last paragraph in two ways[67], by considering the space-time behavior for antiparallel group velocities, and by considering correlation lengths $L_T \sim L_o$. We do so by direct numerical integration of Eqs. (42).

The turbulent part of the wave number mismatch is characterized by amplitude Δ and correlation length L_T. We take the correlation function to be statistically uniform and Gaussian,

$$\langle \delta\kappa(x)\, \delta\kappa(x') \rangle = \Delta^2 \exp\left[-(x - x')^2/2L_T^2\right]. \qquad (65)$$

Since the spectral function $S(k) \equiv \int dy\, e^{iky} \langle \delta\kappa(x)\, \delta\kappa(x + y) \rangle = (2\pi)^{\frac{1}{2}} \Delta^2 L_T \exp(-k^2 L_T^2/2)$, we take as a model* for the random function $\delta\kappa(x)$ a sum of sine waves with random phases,

$$\delta\kappa(x) = (32\pi)^{\frac{1}{2}} \sqrt{\frac{L_T}{L}}\, \Delta \sum_{j=1}^{n=n} \exp\left[-k_j^2 L_T^2/4\right] \sin(k_j x + \alpha_j) \qquad (66)$$

---

* The model mismatch Eq. (66) has a correlation function of the form $\langle \delta\kappa(x)\, \delta\kappa(x') \rangle \sim \sum_j \exp(-k_j^2 L_T^2/2) \cos\left[2\pi j(x - x')/L\right]$ which is periodic in x with period L. For distances of interest $x \ll L$, this correlation function is accurately given by Eq. (65).

where $k_j = 2\pi j/L$; L is an arbitrary basic length, much longer than any other length in the problem; $\{\alpha_j\}$ is a set of random phases, with probability density uniform from zero to 2π; and the upper limit of summation is taken to be large, such that $(k_j L_T)_{MAX} >> 1$. (Of course, care was taken that all turbulent wavelengths be large with respect to the numerical grid spacing. The results are then insensitive to the numerical grid spacing.) For a given realization $\{\alpha_j\}$, and a particular set of parameters, the total mismatch gradient $d\bar{\kappa}(x)/dx = \bar{\kappa}' + d\delta\kappa/dx$ is illustrated in Fig. 13.

Given this model, the coupled-mode equations (42) are integrated numerically to determine the effect of the spatial turbulence on the response of the system to an initial perturbation. The main result of this study is that if Δ exceeds a threshold value (dependent on L_T), the instability no longer saturates at a value $\sim\exp(\pi\lambda)$, but grows exponentially at fixed x for large time, at a growth rate γ lower than that for a nonturbulent homogeneous medium. In Fig. 14 we show the temporal development of a typical unstable case with initial conditions $a_1(x,t=0) = \delta(x)$, $a_2(x,t=0) = 0$. Fluctuations reminiscent of Rosenbluth, White, and Liu[68] are observed, but with a less regular character. The most unstable part of the pulse has the behavior of a temporal normal mode, maintaining its shape while growing exponentially.

In Fig. 15 we show the absolute growth rate γ/γ_o vs Δ/L_o for $V_1/V_2 = -1$, $\lambda^{-1} \equiv \kappa' L_o^2 = 1$, $L_T/L_o = 1.27$. The threshold turbulence level is seen to occur at $\Delta/L_o^{-1} = 0.1$. The maximum growth rate is $\gamma/\gamma_o = 0.70$, which is comparable to the homogeneous growth rate γ_o.

The function $d\kappa(x)/dx$ shown in Fig. 13 corresponds to the threshold case of Fig. 15. This function is seen to lie in the range $0.80 < L_o^2\, d\kappa(x)/dx < 1.20$. This shows that the coupled mode equations can produce absolute instability even if $d\kappa(x)/dx$ vanishes nowhere in the medium, in contrast to the result of Kaw[69] et al.

In Fig. 16 we show the growth rate γ as a function of correlation length L_T, for fixed fluctuation level Δ. For this calculation we use the same realization of the set $\{\alpha_j\}$ in Eq. (2), varying L_T with $\Delta/L_j^{-1} = 0.5$. We see that the absolute growth rate decreases with increasing correlation length.

It should be noted that in this work the turbulent wavelengths are quite long, the shortest being equal to the standard length $L_0 \equiv \sqrt{|v_1 v_2|}/\gamma_o$.

A further point is that for a given value of Δ, the absolute growth rate depends strongly on the realization of $\{\alpha_j\}$ chosen in Eq.(66). The relative dispersion of the growth rates is of the order of 30-40%.

We interpret our results as follows. The convective saturation of the linearly inhomogeneous coupled mode problem[57,68], with oppositely directed group velocities, seems to be due to destructive interferences between responses originating at large positive and negative positions. This interpretation is supported by the work of White[64] et al., who found that replacing the constant pump by a Gaussian in x resulted in absolute instability, as discussed in Section I-B-3; i.e., removing the responses at large x removed the destructive interference at $x = 0$. The analogy in our work is that the turbulence upsets the destructive interferences, allowing the instability to grow absolutely.

We conclude that the presence of long-wave turbulence tends to destabilize the convective saturation found[57,68] for the coupled mode equations, with oppositely directed group velocities, in an inhomogeneous medium. This destabilization occurs at relatively small turbulence levels; so small that the condition $d\kappa(x)/dx$ is never satisfied.

At this time, there exist[71-74] several analytic efforts which deal with situations closely related to this section. Much of this work involves approximations, an example being the Bourret closure approximation, the validity of which are at present being debated.

B. Raman Backscattering in Laser Fusion Model

In this section we apply the results of the previous Section II-A to the question of Raman scattering, in which an electromagnetic wave decays into another electromagnetic wave and a Langmuir oscillation. We consider an example from the parameter regime of laser fusion[97-101].

First studied by Bloembergen and Shen[17], Volkov[18], and Comisar[19], excellent derivations of the coupled mode equations (1) for Raman backscattering are given by Drake[102] et al. and by Liu, Rosenbluth, and White[34]. These derivations proceed from Maxwell's equations and the Lorentz force equation to our Eqs. (42), which are

$$(\partial_t + V_1\partial_x)\, a_1(x,t) = \gamma_0\, a_2(x,t) \exp\left[i\int_0^x \tilde{\kappa}(x')\,dx'\right] \tag{67}$$

$$(\partial_t + V_2\partial_x)\, a_2(x,t) = \gamma_0\, a_1(x,t) \exp\left[-i\int_0^x \tilde{\kappa}(x')\,dx'\right]$$

where a_1 is now the scattered electromagnetic (EM) wave and a_2 is the electron plasma oscillation.

The laser fusion geometry is depicted in Fig. 17, where we see the density rise from zero to above the critical density. Since both decay products have frequencies above the local plasma frequency, $\omega_1 = \sqrt{\omega_p^2 + k_1^2 c^2}$, $\omega_2 = \sqrt{\omega_p^2 + 3k_2^2 v_e^2}$, the pump frequency must satisfy $\omega_o > 2\omega_p$. Thus, Raman scattering can occur only <u>below</u> the point $x_{\frac{1}{4}}$ where $n = n_c/4$, or $\omega_p = \omega_o/2$; the critical density n_c is the density at which $\omega_p = \omega_o$. Furthermore, Raman backscattering can occur only above a certain density, because for too low a density, the Langmuir decay product is strongly Landau damped. We can see this fact as follows. In the far underdense region, $\omega_p(x) \ll \omega_o$, the EM decay product will have a frequency about equal to ω_o, and thus a wavenumber k_1 about equal in magnitude to k_o, but opposite in direction, as shown in Fig. 17. Thus, the Langmuir wave has wavenumber $k_2 \approx 2k_o$. For very low plasma frequency, the Langmuir wave phase velocity $V_\phi \sim \omega_p/2k_o$ will be so small that $k_2\lambda_D \sim 2k_o v_e/\omega_p \sim 1$, producing large Landau damping. In this region, Raman backscatter is suppressed and is dominated by induced Thomson scattering[103], the difference frequency $\omega_o - \omega_1$ now corresponding to a beat disturbance which is not a plasma normal mode in the absence of the pump; the three wave coupled mode equations no longer apply.

We see therefore that Raman instability happens between a minimum density and a maximum density $\frac{1}{4} n_c$, as shown schematically in Fig. 17. Our Eqs. (40) are valid over part of this region, but not all of it. Near the point $x_{\frac{1}{4}}$, the EM wave is near its classical turning point ($\omega_1 \approx \omega_p$) and has $k_1 \approx 0$; thus the wavelength λ_1 is very large and the approximation of slowly varying amplitude $a_1(x,t)$ is no

longer valid; we cannot use Eqs. (42) in this region. We therefore restrict our study to the region indicated schematically in Fig. 17 (Note that we have also neglected damping in Eqs. (67). In practice, the EM wave is collisionally damped, and the Langmuir wave is collisionally and Landau damped. At the end of this section we briefly discuss the effects of damping.)

Let us evaluate the parameters V_1, V_2, γ_o, and $\bar{\kappa}(x)$ in the general vicinity of $\omega_p(x) = \omega_o/3$, or $n(x) = n_c/9$, working to roughly 10% accuracy. We take fixed ω_o and ω_1. For V_1, we have $V_1 = -c\sqrt{1 - \omega_p^2/\omega_1^2} \simeq -c\sqrt{1 - \frac{1}{4}} = -c$. We have $V_2 = 3v_e^2 k_2/\omega_2$, where v_e is the electron thermal speed; we find $k_2 = k_o + |k_1| = \frac{1}{c}\sqrt{\omega_o^2 - \omega_p^2} + \frac{1}{c}\sqrt{\omega_1^2 - \omega_p^2} \simeq (2\omega_o/c)(1 - \omega_p/2\omega_o)$; and $\omega_2 = \omega_o - \omega_1$; thus

$$\frac{V_2}{c} = 3(v_e/c)^2\left(\frac{2\omega_o}{\omega_p} - 1\right) \quad . \tag{68}$$

For γ_o we obtain from Drake[102] et al.

$$\gamma_o = \frac{v_o}{c}\sqrt{\omega_o\omega_p} \tag{69}$$

where v_o is the oscillation velocity of an electron in the field of the pump wave, related to the pump intensity $I(W/cm^2)$ by

$$v_o/c = 10^{-9} I^{\frac{1}{2}} \tag{70}$$

for a Nd:glass laser with $\omega_o = 2\cdot 10^{15}\ s^{-1}$.

Finally, we determine $\bar{\kappa}(x)$. At the point of exact matching x_o, we have $\bar{\kappa}(x_o) = 0$. At any other point, we have $\bar{\kappa}(x) = k_o(x) - k_1(x) - k_2(x)$; expanding about x_o we find

$$\bar{\kappa}(x) = \left(\omega_p^2(x) - \omega_p^2(x_o)\right)$$

$$\left[- \frac{1}{2d\sqrt{\omega_o^2 - \omega_p^2(x_o)}} + \frac{1}{2d\sqrt{\omega_1^2 - \omega_p^2(x_o)}} - \frac{1}{2\sqrt{3}\, v_e \sqrt{\omega_2^2 - \omega_p^2(x_o)}} \right] . \qquad (71$$

For a nonrelativistic plasma, $v_e/c \ll 1$, the Langmuir wave term in Eq.(71) is much larger than the other two terms, yielding

$$\bar{\kappa}(x) = \frac{\omega_p^2(x_o) - \omega_p^2(x)}{2\sqrt{3}\, v_e \sqrt{\omega_2^2 - \omega_p^2(x_o)}} = \frac{\omega_p^2(x_o) - \omega_p^2(x)}{6 v_e^2 k_2} \qquad (72)$$

where all quantities except $\omega_p^2(x)$ are evaluated locally at x_o. In the far underdense region

$$\frac{\bar{\kappa}(x)}{k_o} = \frac{1}{12(k_o\lambda_D)^2} \left[\frac{\omega_p^2(x_o) - \omega_p^2(x)}{\omega_p^2(x_o)} \right] ; \quad \omega_p \ll \omega_o \quad . \qquad (73)$$

For a linear density gradient with scale length L_n, and turbulent relative density fluctuation $\Delta_n(x)$, Eq. (70) becomes, with $x_o = 0$,

$$\bar{\kappa}(x) = \frac{k_2}{6(k_2\lambda_D)^2} \left[\frac{x}{L_n} + \Delta_n(x) \right] \quad . \qquad (74)$$

We choose parameters characteristic of laser fusion[97-101]. The laser is Nd:glass, $\omega_o = 2\cdot10^{15}\ s^{-1}$, $\lambda_o = 1\ \mu m$, intensity $I = 10^{15}\ W/cm^2$, pulse length 100 psec $= 10^{-10}\ s = 2\cdot10^5\ \omega_o^{-1}$. The plasma has $T_e = 1$ KeV, $\omega_p(0) = \omega_o/3$, $\lambda_D = 0.022\ \mu m$, $k_2 = 1.6\ k_o$.

At these values, collisional and Landau damping rates are lower than $\gamma_o = 0.02\ \omega_o$ by a factor of 100. At the homogeneous growth rate, an initial noise level would amplify by $\exp(\gamma_o \times \text{pulse time}) = \exp(0.02\ \omega_o \times 2\cdot10^5\ \omega_o^{-1}) = \exp(4000)$, a huge value which would mean serious attenuation of the incoming laser beam. Thus, it is important to study the inhomogeneous regime, to determine whether such growth rates are actually obtained.

Choosing a density scale length $L_n = 100\ \mu m$, we have from Eqs. (68) and (74)

$$V_1 = -c$$

$$V_2 = 0.03\ c \qquad (75)$$

$$\tilde{\kappa}(x) = 3.3\cdot10^7\ cm^{-2}\ x + 2.8\cdot10^5\ cm^{-1}\ \Delta_n(x) \quad .$$

Also of interest are the parameters $L_o = 1.3\ \mu m$, $\lambda \equiv \gamma_o^2/|V_1V_2|\tilde{\kappa}' = 1.5$. From these we note two important facts. First, we are pushing the WKBJ Eqs. (42) to the limits of their validity, since $L_o = 1.3\ \mu m$ is only slightly larger than $\lambda_o = \lambda_1 = 1.0\ \mu m$; whereas we have assumed $L_o \sim \partial_x \Delta_n|a_1(x,t)| \gg \lambda_o, \lambda_1, \lambda_2$. Secondly, the nonturbulent convective saturation at $\exp(\pi\lambda) = \exp(5)$ is at a very low value for these parameters (for $I = 10^{16}\ W/cm^2$, $\pi\lambda = 50$; for $I = 10^{14}\ W/cm^2$, $\pi\lambda = 0.5$); it is therefore crucial to determine whether turbulence destabilizes the convective saturation, allowing absolute growth.

With $L_T/L_o = 1.3$, and a particular realization of $\{a_j\}$ in Eq. (66), the results are as shown in Fig. 18. Although not shown in Fig. 18, the threshold for absolute instability occurs at a relative RMS density fluctuation $\Delta_n \sim 10^{-4}$ to 10^{-3}, a very low value for real plasmas. The absolute growth rate above threshold is $\gamma/\gamma_o \simeq 0.2$,

falling off for large $\Delta_n^{RMS} \sim 0.1$. This growth rate should be compared to the homogeneous absolute growth rate, which from Eq.(22) is $\gamma/\gamma_o = 2\sqrt{|V_1 V_2|}/(|V_1| + |V_2|) = 0.34$.

The effects of damping on the absolute growth rate have been studied. Results qualitatively similar to those in a homogeneous medium[79] have been found; the growth rate is reduced when the Langmuir wave damping rate $\nu_2 \sim \left|\frac{V_2}{V_1}\right| \gamma_o$.

Thus, we have found that the convective saturation of Raman backscattering in laser fusion geometry is destabilized by very low levels of turbulence, such that the relative RMS density fluctuation is $\Delta_n \sim \sim 10^{-4}$ to 10^{-3}.

Let us depart from the abstract world of one dimensional theory to ask the question: What is the experimental situation regarding Raman backscatter? Answer: There is no direct evidence for any Raman backscatter in any experiment, even though many laser-plasma experiments[104-106] are in the intensity range ($10^{14} - 10^{16}$ W/cm^2 for Nd:glass) where theory predicts huge amounts of Raman scatter. Numerical simulations, however, do demonstrate Raman scattering which behaves as predicted by theory[63,107,108]. There is some indirect experimental evidence for Raman scatter near $\frac{1}{4} n_c$, in that scattered light of frequency $\frac{3}{2}\omega_o$ has been observed[105,106]. Of various theories[109-112] accounting for light at $\frac{3}{2}\omega_o$, all make use of the combination of pump light at ω_o, with Raman or $2\omega_p$ instability-generated radiation at $\omega_o/2$: indeed, a paper by Langdon, Lasinsky, and Kruer[113] shows that at $\frac{1}{4} n_c$, these two instabilities merge into a mixed electrostatic-electromagnetic instability. This is then the indirect evidence for the existence of Raman scattering.

We offer two speculations for the absence of large amounts of Raman backscatter. First, the large turbulence limits of both Fig. 15 and Fig. 18 show a decrease in growth rate for very large turbulence; perhaps such turbulence is experimentally present. Second, it has been shown[114] that magnetic fields associated with turbulence can inhibit Raman scattering; perhaps such magnetic fields are present.

This discussion has been limited to one dimension. There has also been a considerable amount of work on Raman side-scattering[68,70,114-118], which is important since perpendicular to the density gradient the three wave matching conditions can be exactly satisfied over large distances.

III. PARAMETRIC INSTABILITIES IN THE PRESENCE OF A NONMONOTONIC INHOMOGENEITY--A MODEL PROBLEM

A. Theory of Homogeneous Plasma With Sinusoidal Density Modulation

As discussed in part II above, it is very difficult to make analytic progress with our coupled mode equations when the inhomogeneities are nonmonotonic, or turbulent-like. For this reason, we consider the tractable problem of a sinusoidal density inhomogeneity, expressed as a wave number mismatch in the form $\kappa(X) = L_0 \kappa_m \sin(XL_0/L_m)$, the subscript standing for modulation. This problem is like the turbulent problem in two respects: the wave-number mismatch is characterized by an amplitude κ_m and by a length L_m, just as turbulence has an amplitude Δ and a correlation length L_T. This problem is unlike turbulence in one important respect; that is, $\kappa(X)$ is coherent in the sense that the value of the function at each point is given once κ_m and L_m are given. Thus, the solution of this problem will contain important similarities to the turbulent problem, as well as important differences.

We begin with the coupled mode equations in the form

$$\left(\partial_T + \nu_1 + \frac{1}{\sqrt{\beta}}\partial_X\right) a_1(X,T) = a_2(X,T) \exp\left[i\int_0^X \kappa(X')\,dX'\right]$$

$$\left(\partial_T + \nu_2 \pm \sqrt{\beta}\,\partial_X\right) a_2(X,T) = a_1(X,T) \exp\left[-i\int_0^X \kappa(X')\,dX'\right] \qquad (76)$$

where $\beta = |V_2/V_1|$. Assuming a time dependence $a_1(X,T) = a_1(X)\exp(-i\omega T)$, and eliminating the factor

$a_2(X,T)\exp\left[i\int_0^X \kappa(X')\,dX'\right]$ as in section I-C-III above, we have

$$\left\{\partial_X^2 + \left[\pm\frac{1}{\sqrt{\beta}}(-i\omega+\nu_2) - i\kappa(X) + (-i\omega+\nu_1)\sqrt{\beta}\right]\partial_X + \left[\pm(-i\omega+\nu_1)(-i\omega+\nu_2) - i\sqrt{\beta}\,\kappa(X)(-i\omega+\nu_1) \mp 1\right]\right\} a_1(X) = 0 \quad . \tag{77}$$

Assuming that $\kappa(X) = L_o\,\kappa_m \sin(X\,L_o/L_m)$ and defining the new spatial variable $Z \equiv (L_o/L_m)X = x/L_m$, we obtain

$$\left\{\partial_Z^2 + \left(\frac{L_m}{L_o}\right)\left[\pm\frac{1}{\sqrt{\beta}}(-i\omega+\nu_2) + \sqrt{\beta}\,(-i\omega+\nu_1) - iL_o\,\kappa_m\sin(Z)\right]\partial_Z + \left(\frac{L_m}{L_o}\right)^2\left[\pm(-i\omega+\nu_1)(-i\omega+\nu_2) \mp 1 - i\sqrt{\beta}\,(-i\omega+\nu_1) \times L_o\,\kappa_m\sin(Z)\right]\right\} a_1(Z) = 0 \quad . \tag{78}$$

This equation has the simple form

$$\left[\partial_Z^2 + \left(A_1 + A_2\sin(Z)\right)\partial_Z + \left(A_3 + A_4\sin(Z)\right)\right] a_1(Z) = 0 \tag{79}$$

where

$$A_1 = \pm\left(\frac{L_m}{\sqrt{\beta}\,L_o}\right)(-i\omega+\nu_2) + \left(\frac{\sqrt{\beta}\,L_m}{L_o}\right)(-i\omega+\nu_1)$$

$$A_2 = -i\,L_m\,\kappa_m$$

Equation (80) continued next page

Equation (80) continued

$$A_3 = \pm\left(\frac{L_m}{L_o}\right)^2 (-i\omega + \nu_1)(-i\omega + \nu_2) \mp \left(\frac{L_m}{L_o}\right)^2$$

$$A_4 = -i\left(\frac{\sqrt{\beta}\, L_m}{L_o}\right)(-i\omega + \nu_1)\, L_m\, \kappa_m \qquad (80)$$

and where the top sign is for parallel group velocities and the bottom sign is for antiparallel group velocities. When $\omega = 0$, Eq. (79) is equivalent to Ince's equation[119,120]. A simple transformation could then remove the middle term, producing a Hill equation[119,120] of the form $\partial_Z^2 a_1(z) + \left[(c_1 + c_2 \cos(z) + c_3 \cos(2z)\right] a_1(z) = 0$. Only the existence of the $\cos(2z)$ term makes this equation different from the well-known Mathieu equation. For our purposes, the present form Eq.(79) is more convenient.

Equation (79) is periodic in Z with period 2π. Floquet's theorem[119,120] states that there exists a solution of the form

$\exp(kz)\,\phi(z)$ where $\phi(z)$ is periodic in z with period 2π. Such a solution can be very helpful to us, as we shall see below.*

The solution is expressed as

$$a_1(z) = e^{kz}\,\phi(z) = e^{kz} \sum_{n=-\infty}^{\infty} c_n\, e^{inz} \quad ; \qquad (81)$$

---

* Usually, there will be two solutions of Floquet form to Eq. (79), $f_1(z) = \phi_1(z) \exp k_1 z$, $f_2(z) = \phi_2(z) \exp k_2 z$, where ϕ_1 and ϕ_2 are periodic in z with period 2π. If $k_1 \neq k_2$, or $k_1 = k_2$ but $\phi_1(z)$ is linearly independent of $\phi_2(z)$, then $f_1(z)$ and $f_2(z)$ are linearly independent. This is the case in Section III-A-1, where we find $k_2 = -k_1$. For a discrete set of values κ_m, if $\nu_1 = \nu_2 = 0$, we find $k_2 = -k_1 = 0$; in this case it can be shown[119] that $\phi_1(z)$ and $\phi_2(z)$ are indeed linearly independent; $f_1(z)$ and $f_2(z)$ are therefore the complete solution set. In Section III-A-2, the basic Eq. (79) with nonzero ω is more complicated than in Section III-A-1 with $\omega = 0$. Here we force $k_1 = 0$ and solve for ω; this is then one solution of Floquet form $\phi_1(z)$. We remain ignorant of the second solution; there are three possibilities: (i) it could be of Floquet form with different $k_2 \neq 0$; (ii) it could be of Floquet form with $k_2 = 0$ but $\phi_2(z)$ linearly independent of $\phi_1(z)$; (iii) it could be of completely different form. Whichever of these three possibilities occurs is not our concern; we are only interested in determining which values of ω are consistent with a Floquet solution $\exp(k_1 z)\,\phi_1(z)$ having $k_1 = 0$; this we have done.

then Eq. (79) becomes

$$\sum_{n=-\infty}^{\infty}\left[(k + in)^2 + \left(A_1 + \frac{A_2}{2i} e^{iz} - \frac{A_2}{2i} e^{-iz}\right)(k + in)\right.$$

$$\left. + \left(A_3 + \frac{A_4}{2i} e^{iz} - \frac{A_4}{2i} e^{-iz}\right)\right] c_n e^{inz} e^{kz} = 0 \quad . \tag{82}$$

The coefficient of e^{inz} must be zero for each n, $-\infty < n < \infty$; thus we find for each n that

$$\left\{\frac{A_2}{2i}\left[k + i(n-1)\right] + \frac{A_4}{2i}\right\} c_{n-1} + \left\{(k + in)^2 + A_1(k + in) + A_3\right\} c_n$$

$$+ \left\{-\frac{A_2}{2i}\left[k + i(n+1)\right] - \frac{A_4}{2i}\right\} c_{n+1} = 0$$

$$n = \cdots,-2,-1,0,1,2,\cdots \quad . \tag{83}$$

Dividing out the middle coefficient gives a set of equations, which in matrix form would be convergent[119,120]. (An infinite matrix is convergent if (i) the product of the diagonal elements converges, and (ii) the sum of the off diagonal elements converges.) Defining

$$\gamma_n^{\pm} = \frac{\left[A_2 \mp k \mp in - i\right] \mp A_4}{2i\left[(k + in)^2 + A_1(k + in) + A_3\right]} \qquad -\infty < n < \infty \quad . \tag{84}$$

Equations (83) becomes, on dividing out the middle coefficient and using (84),

$$\gamma_n^- c_{n-1} + c_n + \gamma_n^+ c_{n+1} = 0 \qquad -\infty < n < \infty \quad . \tag{85}$$

This set of equations is solved as follows. Defining

$$u_n \equiv \frac{c_{n-1}}{c_n} \quad ; \qquad v_n \equiv \frac{c_{n+1}}{c_n} \quad . \tag{86}$$

Equations (85) become, on dividing through by c_n,

$$\gamma_n^- u_n + 1 + \gamma_n^+ v_n = 0 \qquad -\infty < n < \infty \quad . \tag{87}$$

This set Eqs. (87) can be solved for u_n and v_n, as shown in Appendix F. The result is

$$u_n = -\frac{\gamma_{n-1}^+}{1-}\frac{\gamma_{n-1}^-}{1-}\frac{\gamma_{n-2}^+}{1-}\frac{\gamma_{n-2}^-}{1-}\frac{\gamma_{n-3}^+}{1-}\cdots$$

$$v_n = -\frac{\gamma_{n+1}^-}{1-}\frac{\gamma_{n+1}^+}{1-}\frac{\gamma_{n+2}^-}{1-}\frac{\gamma_{n+2}^+}{1-}\frac{\gamma_{n+3}^-}{1-}\cdots \tag{88}$$

$$-\infty < n < \infty$$

where continued fraction notation has been used, meaning that each minus sign in the denominator acts on everything to the right of it. The solution (81) is now completely determined. The value of k is obtained by choosing a value for n, $n = 0$ let us say, in Eq. (87). Inserting u_o and v_o from (88), and $\gamma_n^{\pm}$ from (84), and A_1, A_2, A_3, A_4 from (80), all into (87) for $n = 0$, we solve for k as a function of ω, K_m, and L_m. That is,

$$\gamma_o^- u_o + 1 + \gamma_o^+ v_o = 0 \tag{89}$$

is a dispersion relation for k. It remains to evaluate c_n, $-\infty < n < \infty$.

The c_n are obtained by choosing a value for c_o, and noting that from the definition (86), we have $c_n = v_o v_1 \cdots v_{n-2} v_{n-1} c_o$ for

$n > 0$, and $c_n = u_o u_{-1} \cdots u_{-n+2} u_{-n+1} c_o$ for $n < 0$. Thus we have constructed the complete solution Eq.(81), aside from an arbitrary constant c_o. In this report we shall not evaluate $\{c_n\}$, but rather obtain as much information as possible from the parameter k.

1. Parallel Group Velocities

As we have seen before, when the group velocities are parallel, $V_1 V_2 > 0$, there is no possibility of absolute instability, and we may consider the problem of the spatial response to a constant source $a_1(X = 0) = 1$, steady state in time. We do this by setting the temporal growth rate $\omega = 0$ in the definition below Eq. (76), and consider Eq. (89) as a dispersion relation for k. For zero modulation κ_m, we know that the spatial response is $\sim \exp(x/L_o)$; for finite modulation we expect this spatial growth rate to be reduced. From Eqs. (80)

$$
\begin{aligned}
A_1 &= \frac{2 L_m}{\sqrt{\beta}\, L_o} + \frac{\nu_1 \sqrt{\beta}\, L_m}{L_o} \\
A_2 &= -i L_m K_m \\
A_3 &= (\nu_1 \nu_2 - 1)(L_m/L_o)^2 \\
A_4 &= -i \nu_1 (L_m K_m)(\sqrt{\beta}\, L_m/L_o) \quad .
\end{aligned}
\tag{90}
$$

Then from Eqs. (84) we have

$$
\gamma_n^{\pm} = \frac{-(L_m K_m)\left[\mp k \mp in - i \mp \nu_1 \sqrt{\beta}\, L_m/L_o\right]}{2\left[(k+in)^2 + (k+in)(L_m/L_o)(\nu_1 \sqrt{\beta} + \nu_2/\sqrt{\beta}) + (L_m/L_o)^2(\nu_1 \nu_2 - 1)\right]}
$$

$$
-\infty < n < \infty \quad . \tag{91}
$$

For small $L_m\kappa_m$, we can approximate u_o, v_o in Eq. (89) by the first term in the expressions (88), all other terms being proportional to higher powers of $L_m\kappa_m$. Then Eq. (89), our dispersion relation, becomes

$$-\gamma_o^- \gamma_{-1}^+ - \gamma_o^+ \gamma_{+1}^- + 1 = 0 \quad . \tag{92}$$

For heuristic clarity, set $\nu_1 = \nu_2 = 0$, $\beta = 1$. Then Eq. (92) is

$$\frac{(\kappa_m L_m)^2 k(k-1)}{4(k^2 - L_m^2/L_o^2)\left[(k-1)^2 - L_m^2/L_o^2\right]} + \frac{(\kappa_m L_m)^2 k(k+1)}{4(k^2 - L_m^2/L_o^2)\left[(k+1)^2 - L_m^2/L_o^2\right]} + 1 = 0 \quad . \tag{93}$$

For fixed L_m, let $\kappa_m \to 0$. Then Eq. (93) can be satisfied only if the denominator in one of the terms vanishes. Choosing $k^2 - L_m^2/L_o^2 = 0$ yields $k = \pm L_m/L_o$, or $a_1(x) \sim \exp\left[\pm \frac{L_m}{L_o} z\right] \sim \exp\left[\pm X\right] \sim \exp\left[\pm x/L_o\right]$, the usual result for a homogeneous medium. The other zeros of the denominators yield $k = L_m/L_o \pm 1$; but this is the same as above since $\exp\left[\pm iz\right]$ is periodic with period 2π and so can be absorbed in $\phi(z)$ in Eq. (81). In fact, a careful look at the full dispersion relation (89) shows that for $\kappa_m \to 0$, there are an infinite number of roots $k = \pm L_m/L_o + i\ell$, $-\infty < \ell < \infty$, all of them equivalent to the $\ell = 0$ root.

For small $\kappa_m L_m$, we expand about $k \simeq L_m/L_o$, and solve Eq. (93) for the small quantity $(k - L_m/L_o)$; we find in physical units the inverse growth length $L^{-1} = \frac{k}{L_m}$, which is

$$L^{-1} = k/L_m = L_o^{-1}\left[1 - \frac{(\kappa_m L_m)^2}{4\left(1 + 4L_m^2/L_o^2\right)}\right]; \qquad \kappa_m L_m << 1 \quad . \quad (94)$$

Thus, for small modulation amplitude κ_m the growth length is increased by a term proportional to κ_m^2. The increase in growth length is most pronounced for large modulation wavelength L_m.

For arbitrary κ_m, we can solve Eq. (89) numerically for the inverse growth length k, keeping as many terms as necessary in the continued fractions of Eq. (88) for u_o and v_o. The results are shown in Fig. 19 for $L_m/L_o = 1$, and in Fig. 20 for $L_m/L_o = 0.5$. The spatial growth rate, in units of the zero modulation spatial growth rate L_o^{-1}, decreases with increasing modulation κ_m until a certain point, where it reaches zero and bounces up again. For completeness, we have shown both the positive and the negative roots; both roots are purely real. We interpret the bouncing effect as being due to constructive and destructive interferences between the oppositely traveling solutions to our second order differential equation (77).

2. Antiparallel Group Velocities

If $V_1V_2 < 0$, it is no longer appropriate to consider a steady state in time, so we consider a different, physically relevant problem. We ask the question: What is the temporal response of the system to the uniform initial conditions $a_1(x,t = 0) = \text{constant}$, $a_2(x,t = 0) = 0$? We expect to find a temporal growth rate $\text{Im}(\omega)$ which in the limit $\kappa_m \to 0$ reduces to the usual homogeneous result $\text{Im}(\omega) = 1$ (or in physical units, $\text{Im}(\omega) = \gamma_o$). The basic equations (76) are periodic, and the initial conditions are periodic; thus,

we may look for a periodic solution to Eqs. (79) which means setting $k = 0$ in Eq. (81). Then Eq. (89) becomes a dispersion relation for ω, with k set equal to zero.

In this case, we have from Eqs. (80)

$$
\begin{aligned}
A_1 &= -\frac{L_m}{\sqrt{\beta}\,L_o}(-i\omega+\nu_2) + \frac{\sqrt{\beta}\,L_m}{L_o}(-i\omega+\nu_1) \\
A_2 &= -iL_m\kappa_m \\
A_3 &= -(L_m/L_o)^2(-i\omega+\nu_1)(-i\omega+\nu_2) + (L_m/L_o)^2 \\
A_4 &= -i(\sqrt{\beta}\,L_m/L_o)(-i\omega+\nu_1)L_m\kappa_m \quad .
\end{aligned}
\tag{95}
$$

Using (84) and (95) we have

$$
\gamma_n^{\pm} = \frac{(L_m\kappa_m/2)\left[(\mp in-1) \mp (\sqrt{\beta}\,L_m/L_o)(-i\omega+\nu_1)\right]}{\left\{n^2 - in\left[-\frac{L_m}{\sqrt{\beta}L_o}(-i\omega+\nu_2) + \frac{\sqrt{\beta}L_m}{L_o}(-i\omega+\nu_1)\right] + \left(\frac{L_m}{L_o}\right)^2(-i\omega+\nu_2)(-i\omega+\nu_1) - \left(\frac{L_m}{L_o}\right)^2\right\}} . \tag{96}
$$

For small $(\kappa_m L_m)$, we again choose only the first term in the expressions (88) for u_o, v_o and again obtain the simplified dispersion relation (92). For simplicity, set $\beta = 1$ $(V_1 = -V_2)$, and $\nu_1 = \nu_2 = 0$. Then we find, as expected, that for $\kappa_m L_m \to 0$ the temporal growth rate is $\mathrm{Im}(\omega) = 1$ $[\mathrm{Im}(\omega) = \gamma_o$ in physical units . For small $\kappa_m L_m$, we find

$$
\mathrm{Im}(\omega) = 1 - \frac{\kappa_m^2 L_m^2}{4} \qquad \kappa_m L_m \ll 1 \quad . \tag{97}
$$

The decrease in temporal growth rate is proportional to κ_m^2, and is most pronounced for large modulation wavelengths L_m.

Let us note that in addition to the root discussed in the previous paragraph, there are an infinite number of other roots. To see this, first consider the form of $\gamma_n^{\pm}$ in Eq. (96) when $\beta = 1$, $\nu_1 = \nu_2 = 0$, which is

$$\gamma_n^{\pm} = \frac{(L_m\kappa_m/2)\left[\pm in - 1 \pm i\omega L_m/L_o\right]}{n^2 - (L_m/L_o)^2(\omega^2 + 1)} . \tag{98}$$

Next, consider the form of the full dispersion relation (89) which is, after inserting u_o and v_o from Eqs. (88),

$$\left\{ - \frac{\gamma_o^- \gamma_{-1}^+}{1^-} \frac{\gamma_{-1}^- \gamma_{-2}^+}{1^-} \cdots \right\} + 1 + \left\{ - \frac{\gamma_o^+ \gamma_1^-}{1^-} \frac{\gamma_1^+ \gamma_2^-}{1^-} \cdots \right\} = 0 . \tag{99}$$

Since each $\gamma_n^{\pm}$ has κ_m in the numerator, the only way to satisfy the dispersion relation (99) when $\kappa_m \to 0$ is to make one of the denominators in (99) vanish also. This occurs for

$$\omega = \pm (n^2 L_o^2/L_m^2 - 1)^{\frac{1}{2}} \qquad \begin{matrix} L_m\kappa_m \to 0 \\ n = 0,1,2,\cdots \end{matrix} . \tag{100}$$

This infinite set of roots is reminiscent of the theory of wave propagation in periodic media, where we find an infinite number of roots $\omega(k = 0)$, one root per Brillouin zone[121]. For finite κ_m, we expect one branch of the graph ω vs κ_m associated with each root (100). In the special case $\beta = 1$, $\nu_1 = \nu_2 = 0$, it is easy to show from Eqs. (98) and (99) that if ω is a root of (99) for given κ_m, then so is $-\omega$ and so is $-\omega^*$.

The grant from UNESCO, and the financial support of Lawrence Berkeley Laboratory are gratefully acknowledged.

This work was performed under the auspices of the United States Atomic Energy Commission.

B. Linear Density Gradient With Sinusoidal Density Modulation

We consider next a sinusoidal density modulation in the presence of a linear density gradient. We restrict ourselves to antiparallel group velocities, and take the wave number mismatch to be

$$\kappa(X) = \kappa' X + (L_o \kappa_m) \sin(XL_o/L_m) \quad . \tag{102}$$

For small κ_m, we expect to recover the usual $\exp(\pi/\kappa')$ saturation discussed in Section I-E. For larger κ_m, we might expect to destabilize the convective saturation, just as turbulence did in Section II.

We numerically integrate the basic equations (76) with the form (102) for $\kappa(X)$ and with Green's function initial conditions. We indeed find $\exp(\pi/\kappa')$ saturation for small κ_m, and we indeed find absolute instability for κ_m greater than an L_m-dependent threshold. In Fig. 22 we show the absolute growth rate, obtained with $B = \kappa' = 1$, $L_m/L_o = 0.8$. Above threshold, the growth rate rises rapidly to nearly the homogeneous medium growth rate.

In the example shown in Fig. 22, the threshold value of κ_m occurs at $L_o\kappa_m = 0.1$. As in the turbulent case of Section II, this value of $L_o\kappa_m$ is far below that required for the vanishing of the derivative of the wave number mismatch $\kappa(X)$; i.e., $d\kappa(X)/dX = \kappa' + (L_o^2\kappa_m/L_m)\cos(XL_o/L_m) = 0$ implies (with $\kappa' = 1$ and $L_m/L_o = 0.8$) that $L_o\kappa_m = 0.8$, a much higher value of $L_o\kappa_m$ than the observed threshold $L_o\kappa_m \approx 0.1$.

We next consider a shorter wavelength modulation, $L_m/L_o = 0.18$, in Fig. 23. Here we see a much less violent instability, the maximum growth rate being only $\mathrm{Im}(\omega)/\gamma_o \approx 0.2$. Furthermore, the threshold value of κ_m is $L_o\kappa_m = 1.0$, much higher than would be predicted by setting $d\kappa(x)/dx = 0$, yielding here $L_o\kappa_m = 0.18$.

Our conclusion from the last two paragraphs is that the modulation wavelength is the relevant parameter in determining the tendency of the system toward absolute instability, rather than considerations of the vanishing of the derivative of the wave number mismatch $K(X)$. This conclusion is emphasized in Fig. 24, where we hold the modulation amplitude fixed at a value $L_o\kappa_m = 2(\beta = \kappa' = 1)$ and vary the modulation wavelength. We find that the absolute growth rate is substantial for $L_m \sim L_o$, falling off rapidly for $L_m \ll L_o$ and for $L_m \gg L_o$.

In Fig. 25, we display the results of Figs. 22, 23, 24 as a three dimensional plot of absolute growth rate γ vs κ_m and L_m. The dashed curve is schematic, showing the inferred threshold for absolute instability in the K_m-L_m plane. For large κ_m, the threshold value of L_m approaches zero. For both large and small L_m, the threshold value of κ_m is large, demonstrating once again that the most effective inhomogeneities are those with scale length $\sim L_o$.

We again interpret these results in terms of the concept of mathematical reflections discussed in Appendix A. When the inhomogeneities are of a size near the all important length L_o, constructive interferences between solutions of our second order system Eqs. (76) lead to instability. When the inhomogeneities are of a size much smaller or greater than L_o, the system feels only the monotonic part of $\kappa(X)$, given by $\kappa' X$, and exhibits the usual $\exp(\gamma/\kappa')$ saturation. This saturation we interpret as a destructive interference between solutions of our second order set Eqs. (76).

The detailed space-time response of the system, to the initial conditions $\psi_1(X,T = 0) = \delta(X)$, $\psi_2(X,T = 0) = 0$, is of interest in its own right. For the parameters of Fig. 24 ($L_o\kappa_m = 2$, $\beta = \kappa' = 1$) we choose a value for the modulation wavelength, $L_m/L_o = 0.16$,

which is just barely above the threshold for absolute instability. Figure 26 shows the space-time behaviour of $a_2(X,T)$ at four different times, $T = 7,13,16,20$. At $T = 7$, the usual $\exp(\pi/\kappa')$ saturation has set in. At the substantially later time $T = 13$, the $\exp(\pi/\kappa')$ behavior persists, but with many more fluctuations. The hint of things to come is shown by the enhanced fluctuation at $X = 0$, in the middle of the figure. At $T = 16$, this enhanced fluctuation has grown rapidly to tower over the rest of the pulse shape. After a period of rapid growth, the enhanced fluctuation at $X = 0$ itself saturates. This saturated state, shown at $T = 20$, has its own enhanced fluctuations at the very center which foretell the outburst of yet a third period of rapid growth, and so on ad infinitum.

To conclude, we have seen that the behavior of the system of Eqs. (76) with the wave number mismatch $\kappa(X) = \kappa'X + (L_o\kappa_m)\sin(XL_o/L_m)$ is qualitatively similar to the turbulent case of Section II. Absolute instability results for wavelengths $L_m \sim L_o$, and for modulation amplitudes one order of magnitude smaller than that required to make $d\kappa(X)/dX = 0$. The instability growth rate is very sensitive to modulation wavelength L_m, falling off rapidly for $L_m \ll L_o$.

ACKNOWLEDGMENTS

Words are insufficient to express my gratitude to my advisor, Allan Nathan Kaufman. From my first day in Berkeley, his uncompromising excellence in teaching and in research has been a constant inspiration. To paraphrase the law professor in the movie "Paper Chase", he has taken "the mush between my ears" and turned it into the mind of a scientist.

To my lover Jane is due the credit for keeping me human, while becoming a scientist. I am grateful for her continuous encouragement and patience.

Many thanks are due to my fellow graduate students Bruce Cohen, Mike Mostrom, and Gary Smith, for stimulating discussions and helpful advice through these years.

I am grateful to C. K. Birdsall for teaching me the art of computer simulation, and for advice and guidance in my early years of research.

I have greatly benefited from contact with our two postdocs, Claire Max and Shayne Johnston. Their professional competence was always a good example for my own work.

This thesis could not have been written without the goodwill and assistance of Georgella Perry and Christina Graham. Georgella's mastery of the laboratory bureaucracy is a great simplifier of life, as her afternoon cookies are a great sustainer of life. To Chris go the thanks for starting each morning with a few words of friendly conversation, as well as a cup of her good coffee, about 5000 cups of which have gone into this thesis.

For tenderly guiding me through the requirements of the Physics Department, thanks are due to Teri Doizaki, the best friend a graduate student could have.

This work was supported by the U. S. Energy Research and Development Administration.

APPENDICES

A. The Concept of Reflections

Bobroff and Haus have treated the case of homogeneous medium, finite pump length (Sec. I-B-2) in several different ways. One of them uses the concept of "reflections". Consider Eqs. (25), with $D_1 = D_2 = 0$, $V_2/V_1 = -1$, which are

$$\begin{aligned} (\partial_T + \partial_X)\, a_1(X,T) &= a_2(X,T) \\ (\partial_T - \partial_X)\, a_2(X,T) &= a_1(X,T) \,. \end{aligned} \tag{A.1}$$

Using the method of characteristics we define new variables

$$\begin{aligned} y &\equiv T - X \\ z &\equiv T + X \,. \end{aligned} \tag{A.2}$$

Equations (A.1) become

$$\begin{aligned} \partial_z\, a_1(y,z) &= \tfrac{1}{2}\, a_2(y,z) \\ \partial_y\, a_2(y,z) &= \tfrac{1}{2}\, a_1(y,z) \,. \end{aligned} \tag{A.3}$$

Eliminating a_2 from Eqs. (A.3) we have

$$\partial_{yz}^{\,2}\, a_1(y,z) = \tfrac{1}{4}\, a_1(y,z) \,. \tag{A.4}$$

From the symmetry of Eq. (A.4) we see that if $f(y,z)$ is a solution, then $f(z,y)$ is also a solution. Referring to Fig. 2, we perturb the system at some point x_o, $0 < x_o < L$. Assume that the solution $f(y,z)$ has been excited by our perturbation; then the solution $f(y,z)$ will propagate (in X and T) as in an infinite medium until

one edge reaches one of the boundaries $X = 0$ or $X = L/L_o$. Assume it reaches $X = 0$ first. With $V_1 > 0$, we have the boundary condition $a_1(X = 0,T) = 0$. Now at $X = 0$, $y = z = T$, so that $f(y,z) = f(r,y)$ at $X = 0$ for all T. Thus, after the pulse reaches the boundary, the solution $a_1(X,T) = f(y,z) - f(z,y)$ satisfies the boundary conditions; this solution looks like the original solution $f(y,z)$ plus a reflected solution. This argument can be continued in time so that each time one solution reaches a boundary, a new solution is brought in; the response is thus seen as a sum of repeated reflections.

B. Sudan's Criterion for Absolute Instability in Inhomogeneous Media

In an early paper[87], Sudan proposed, without proof, a generalization to inhomogeneous media of the Bers-Briggs criterion[78] for absolute instability. In a homogeneous medium, a necessary (not sufficient) condition for absolute instability is that there be a saddle point of the phase $i(\omega t - k(\omega)x)$ in the complex ω-plane, where $k(\omega)$ is obtained from the dispersion relation $D(k,\omega) = 0$.

$$\frac{\partial}{\partial\omega}\left[\omega t - k(\omega)x\right] = 0 \Rightarrow \frac{\partial k(\omega)}{\partial\omega}\, x = t \quad . \tag{A.5}$$

For asymptotic time at a fixed position x_o

$$\frac{\partial k(\omega)}{\partial\omega} \to \infty \tag{A.6}$$

the solution of which determines the unstable frequency ω_a.

In an inhomogeneous medium, the phase has the form

$$\exp i\left[\omega t - \int_0^x k(\omega;\, x')\, dx'\right] \tag{A.7}$$

where $k(\omega;x)$ is obtained from the dispersion relation

$$D(k,\omega;\, x) = 0 \ . \tag{A.8}$$

Then the saddle point condition at a point x_o becomes

$$\int_0^{x_o} \frac{\partial k(\omega;\, x')}{\partial \omega}\, dx' = t \to \infty. \tag{A.9}$$

We determine $D(k,\omega;\, X)$ from the dimensionless Eqs.(4.), taking $V_2/V_1 = -1$; then

$$\left[\partial_T - \partial_X + i\kappa(X)\right]\left[\partial_T + \partial_X\right] a_1(X,T) - a_1(X,T) = 0 \ . \tag{A.10}$$

Fourier transforming locally (not affecting $\kappa(X)$) we find

$$\left[\omega + k + \kappa(X)\right]\left[\omega - k\right] + 1 = 0 \ . \tag{A.11}$$

Solving Eq. (A.11) for $k(\omega;\, X)$ and $\partial_\omega\, k(\omega;\, X)$ we find

$$\partial_\omega\, k(\omega;\, X) = \pm(2\omega + \kappa)\left[\left(\frac{\kappa(X)}{2}\right)^2 + 1 + \omega^2 + \omega\kappa(x)\right]^{-\frac{1}{2}} \ . \tag{A.12}$$

In order to have $\int_0^{x_o} \partial_\omega\, k(\omega;\, x')\, dx' \to \infty$, as required by Eq. (A.9), we must have $\partial_\omega\, k(\omega;\, X)\big|_{X=X_o} \to \infty$, since the lower limit of integration is arbitrary. We therefore require the denominator in Eq. (A.12) to vanish at $X = X_o$; taking $X = X_o$ to be the point where $\kappa(X)$ vanishes (we can always add a constant to $\kappa(X)$ to make this be true),

we find the unstable frequency $\omega = i$. In the neighborhood of $X = X_0$, Eq. (A.12) has the form

$$\partial_\omega k(\omega; X) = \frac{1}{\left[\frac{\kappa^2(X)}{4} + i\kappa(X)\right]^{\frac{1}{2}}} . \qquad (A.13)$$

Assuming a power law form for $\kappa(X)$

$$\kappa(X) \sim (X - X_0)^N \qquad (A.14)$$

we have near $X = X_0$

$$\partial_\omega k(\omega; X) \sim (X - X_0)^{N/2} . \qquad (A.15)$$

Condition (A.9) then becomes $\int_0^{X_0} (X' - X_0)^{-N/2} dX' \to \infty$, which will be true only for $N \geq 2$. This agrees precisely with the results of Rosenbluth[57], who found no absolute instability for $\kappa(X) \sim X$; and an absolute instability with growth rate $\gamma/\gamma_0 \approx 1$ for $\kappa(X) \sim X^2$.

However, this method does not agree with our results for the turbulent case, Sec. II, or for the case $\kappa(X) = \kappa' X + L_0 \kappa_m \sin(XL_0/L_m)$, Sec. III. For these cases, absolute instability is found when $d\kappa(X)/dX$ vanishes nowhere in the system, and condition (A.9) is never satisfied. Thus, Sudan's method works for monotonic inhomogeneities, but not for turbulent like inhomogeneities.

C. Analytic Solution for the Case of Finite Pump, Inhomogeneous Plasma

At some point it may prove useful to have an exact analytic solution for the case of finite pump extent, inhomogeneous plasma. Referring to Fig. 8, we wish to solve Eqs. (43), which are

$$(\partial_t + \nu_1 + V_1\partial_x)\, a_1(x,t) = \gamma_0\, a_2(x,t)\exp(i\bar{\kappa}'x^2/2)$$
$$(\partial_t + \nu_2 + V_2\partial_x)\, a_2(x,t) = \gamma_0\, a_1(x,t)\exp(-i\bar{\kappa}'x^2/2) \qquad (A.16)$$

for $V_1 > 0$, $V_2 < 0$; with the boundary conditions $a_1(x = 0,t) = a_2(x = L,t) = 0$; and with the initial conditions $a_1(x,t = 0) = 0$, $a_2(x,t = 0) = \delta(x - x_0)$, $0 \le x_0 \le L$. We follow Rosenbluth, White, and Liu[60], who solved the infinite pump extent case. After a similar calculation, we find

$$a_1(x,t) = \frac{1}{2\pi}\int_L e^{pt}\, a_1(x,p)\, dp \qquad (A.17)$$

where the integral is taken around the Laplace contour, and must satisfy causality: $a_1(x,t < 0) = 0$. $a_1(x,p)$ is given by

$$a_1(x,p) = a(x,p)\, e^{-i\bar{\kappa}'x^2/4}\, e^{-\left[\frac{p+\nu_1}{V_1}\wedge\frac{p+\nu_2}{V_2}\right]\left(\frac{\pi}{2}\right)} \qquad (A.18)$$

$$a(x,p) = \frac{\lambda}{\gamma_0}\, e^{\pi\lambda/2}\, e^{i\pi/4}$$
$$\times \left\{\frac{a_+(x,p)\, a_-(x_0,p)\, \theta(x - x_0) + a_+(x_0,p)\, a_-(x,p)\, \theta(x_0 - x)}{F_+(p) - F_-(p)}\right\}$$

where $\lambda \equiv \gamma_0^2/\bar{\kappa}'|V_1V_2|$,

$$\theta(x) = \begin{cases} 1 & x \ge 0 \\ 0 & x < 0 \end{cases} .$$

The functions a_+, a_-, F_+, F_- are defined by

$$a_+(x,p) = F_+(p)\, D_{-i\lambda}(x' e^{i\pi/4}) + D_{i\lambda-1}(-x' e^{-i\pi/4})$$

$$a_-(x,p) = F_-(p)\, D_{-i\lambda}(x' e^{i\pi/4}) + D_{i\lambda-1}(-x' e^{-i\pi/4}) \qquad \text{(A.19)}$$

$$F_+(p) = \frac{i\bar{\kappa}' L D_{-i\lambda}(x_L' e^{i\pi/4}) + i\lambda V_1 \sqrt{\bar{\kappa}'}\, e^{i\pi/4} D_{-i\lambda-1}(x_L' e^{i\pi/4})}{\left[\left\{p + \nu_1 + (p + \nu_2)V_1/V_2\right\} D_{i\lambda-1}(-x' e^{-i\pi/4}) - V_1\sqrt{\bar{\kappa}'}\, e^{-i\pi/4}(i\lambda - 1)\, D_{i\lambda-2}(-x_L' e^{-i\pi/4})\right]}$$

$$F_-(p) = -D_{i\lambda-1}(-x_o' e^{-i\pi/4})$$

where

$$x' \equiv \sqrt{\bar{\kappa}'}\, x - \frac{1}{\sqrt{\bar{\kappa}'}}\left(\frac{p + \nu_1}{V_1} + \frac{p + \nu_2}{V_2}\right) ,$$

$$x_o' \equiv (x')_{x=0} ;$$

$$x_L' \equiv (x')_{x=L}$$

and where $D_\nu(z)$ is the parabolic cylinder function[122]. For $\mathrm{Re}[\nu] < 0$

$$D_\nu(z) = \frac{e^{-z^2/4}}{\Gamma(-\nu)} \int_0^\infty dt\, e^{-t^2/2 - zt}\, t^{-\nu-1} \qquad \text{(A.20)}$$

$$\frac{|z| >> |\nu|}{|z| >> 1}\ e^{-z^2/4}\, z^\nu .$$

It is clear that this solution must be evaluated numerically. We have found it easier in practice to integrate Eqs. (41) directly to obtain the Green's function shown in Fig. 10.

D. Numerical Integration Using the Method of Characteristics

We discuss the details of the numerical integration of our coupled mode equations.

Consider the most general coupled mode Eqs. (40), written in the form

$$\begin{aligned} (\partial_t + V_1\partial_x)\, a_1(x,t) &= f_1(x,t) \\ (\partial_t + V_2\partial_x)\, a_2(x,t) &= f_2(x,t) \end{aligned} \tag{A.21}$$

where $f_1(x,t)$ $f_2(x,t)$ are functions of (x,t) and functionals of $a_1(x,t)$, $a_2(x,t)$, $\nu_0(x)$, and $\bar{n}(x)$. Equations (A.26) are an example of a hyperbolic system of equations, so long as at least one of V_1, V_2 is different from zero. Numerical solution of Eqs. (A.21) is facilitated by use of the method of characteristics[123]. Defining the variables

$$\begin{aligned} \eta &\equiv x - V_1 t \\ \xi &\equiv x - V_2 t \quad . \end{aligned} \tag{A.22}$$

Equations (A.21) become

$$\begin{aligned} \partial_\xi a_1 &= \frac{f_1(\eta,\xi)}{V_1 - V_2} \\ \partial_\eta a_2 &= \frac{f_2(\eta,\xi)}{V_2 - V_1} \quad . \end{aligned} \tag{A.23}$$

Each equation now has only one derivative. In the x-t plane, the situation is shown in Fig. 27. Starting at the point ($x = 0$, $t = 0$) we draw a line of constant $\eta \equiv x - V_1 t$ ($\eta = 0$ for this line) and a line of constant $\xi \equiv x - V_2 t$ ($\xi = 0$ for this line). The slope of the first is $\Delta t/\Delta x = \frac{1}{V_1}$; the slope of the second is $\Delta t/\Delta x = 1/V_2$ (assume $V_2 < 0$). Marking off the time axis at intervals Δt, we define a grid point on each line of constant η or ξ, at intervals Δt above the x axis. From each grid point comes a new line of constant η or ξ, called characteristic lines.

Next we put Eqs. (A.28) in finite difference form

$$\frac{\Delta a_1}{\Delta \xi} = \frac{f_1(\eta,\xi)}{V_1 - V_2}$$

$$\frac{\Delta a_2}{\Delta \eta} = \frac{f_2(\eta,\xi)}{V_2 - V_1} \quad . \tag{A.24}$$

Suppose we know all values $a_1(\eta,\xi)$, $a_2(\eta,\xi)$ on the horizontal line at $t = 3\Delta t$, for example, and we wish to know the values of a_1, a_2 along the horizontal line at $t = 4\Delta t$. At points α,β in Fig. 27, we know $a_1(\alpha)$, $a_2(\alpha)$, $a_1(\beta)$, $a_2(\beta)$ and we desire $a_1(\gamma)$, $a_2(\gamma)$, where $a_1(\alpha) \equiv a_1(\eta$ at point α, ξ at point $\alpha)$, etc. We use a predictor-corrector method[123], accurate to first order in Δt. Working from Eq. (A.29), we predict a value $a_1(\gamma)_p$ for $a_1(\gamma)$ as follows:

$$a_1(\gamma)_p = a_1(\alpha) + \Delta\xi\, f_1(\alpha)/(V_1 - V_2)$$

$$a_2(\gamma)_p = a_2(\beta) + \Delta\eta\, f_2(\beta)/(V_2 - V_1) \quad . \tag{A.25}$$

Note that we are integrating along characteristics, and that only information at α,β is necessary to predict a value at γ.

We now correct our predicted values, defining corrected values for $a_1(\gamma)_c$, $a_2(\gamma)_c$ as follows:

$$a_1(\gamma)_c = a_1(\alpha) + \frac{1}{2}\frac{\Delta\xi}{(V_1 - V_2)}\left(f_1(\alpha) + f_1(\gamma)_p\right)$$

$$a_2(\gamma)_c = a_2(\beta) + \frac{1}{2}\frac{\Delta\eta}{(V_2 - V_1)}\left(f_2(\beta) + f_2(\gamma)_p\right) \quad . \tag{A.26}$$

We define $\epsilon \equiv \left[a_1(\gamma)_c - a_1(\gamma)_p\right]/a_1(\gamma)_p$; if ϵ is small enough we are done, setting $a_1(\gamma) = a_1(\gamma)_c$, $a_2(\gamma) = a_2(\gamma)_c$. If ϵ is not yet small enough, we set $a_1(\gamma)_p = a_1(\gamma)_c$, $a_2(\gamma)_p = a_2(\gamma)_c$; insert the new predicted values into (A.26); obtain a new $a_1(\gamma)_c$, $a_2(\gamma)_c$; test ϵ again; and so on until ϵ is small enough.

In practice, this technique works well and economically. For the dimensionless Eqs.(30), with $\beta = 1$, theory predicts $\gamma = 1$; numerically the relative error in γ is approximately equal to Δt.

E. An Example Where WKBJ Theory Is No Better Than It Should Be

WKBJ theory[86] has a reputation for having, in many instances, a much wider range of validity than its derivation would indicate. Here we demonstrate a situation where the WKBJ solution has only the minimum range of validity.

In Section III-A-1, we considered the steady state, spatial growth rate when

$$\kappa(X) = L_o\kappa_m \sin(XL_o/L_m) \tag{A.27}$$

for which Eqs. (III-1) are (taking $\beta = 1$)

$$\partial_X a_1 = a_2 \exp i \int_0^X L_o\kappa_m \sin(X'L_o/L_m)\, dX'$$

$$\partial_X a_2 = a_1 \exp -i \int_0^X L_o\kappa_m \sin(X'L_o/L_m)\, dX' \quad . \tag{A.28}$$

In certain limits it is not necessary to use the complicated analysis of Section III-A to find the growth length. We can instead use the WKBJ solution of Eqs. (A.28). Putting (A.28) in the form

$$\partial_X^2 a(X) + q(X)\, a(X) = 0 \tag{A.29}$$

where $a(X) \equiv a_1(X) \exp\left[-\frac{1}{2}\int_0^X L_o\kappa_m \sin(X'L_o/L_m)\, dX'\right]$ we find for $q(X)$,

$$q(X) = -1 + \frac{1}{2} L_o^2\kappa_m/L_m \cos\left(\frac{XL_o}{L_m}\right) + \frac{1}{4}(L_o\kappa_m)^2 \sin^2\left(\frac{XL_o}{L_m}\right) \quad . \tag{A.30}$$

WKBJ theory[86] assigns two approximate solutions to (A.29), which are

$$f(X) = \frac{1}{4\sqrt{q(X)}} \exp\left[\pm 1 \int_0^X \sqrt{q(X')}\, dX'\right] \tag{A.31}$$

valid if $q(X)$ is not close to zero. Expanding $\sqrt{q(X)}$ for small $(L_o\kappa_m)$, and integration over a distance large compared to L_m, we find a growth length

$$L_o/L_g = \cdots - \left(\frac{L_m\kappa_m}{4}\right)^2\left[\left(\frac{L_o}{L_m}\right)^2 - \frac{1}{4}\left(\frac{L_o}{L_m}\right)^4\right] \qquad (A.32)$$

which is incorrect for arbitrary L_o/L_m; it reduces to the correct value Eq. (III-19) only in the limit $L_o/L_m \ll 1$, where we find

$$L_o/L_g = 1 - \frac{(L_m\kappa_m)^2}{4\left(1 + 4(L_m/L_o)^2\right)} \qquad . \qquad (A.33)$$

Why is it necessary to go to the $L_o/L_m \ll 1$ limit to get the correct growth length? The answer lies in the position of the zeros of $q(X)$, which for small $(L_o\kappa_m)$ occur at

$$X_n = \pm\frac{L_m}{L_o}\left(\frac{n\pi}{2}\right) \pm i\left(\frac{L_m}{L_o}\right)\ln\left[\frac{4L_m/L_o}{L_o\kappa_m}\right] \qquad n = 1,5,9,\cdots \qquad . \qquad (A.34)$$

Thus, the zeros of $q(X)$ are far from the real X axis only when $L_m/L_o \gg 1$ (because of the log dependence on $L_o\kappa_m$, it is not sufficient to have $L_o\kappa_m \ll 1$); the WKBJ solutions (A.31) are thus valid on the real axis only for $L_m/L_o \gg 1$, when the roots of $q(X)$ are far from the real axis. For $L_m/L_o \lesssim 1$, the roots of $q(X)$ are near the real axis and the WKBJ solution (A.31) is incorrect. This is an example where WKBJ theory works only where it should, that is, in regions of the complex X-plane far from zeros of $q(X)$.

F. The Solution of an Infinite Set of Algebraic Equations

We wish to solve the infinte set of coupled Eqs.(A.27), which are

$$\gamma_n^- c_{n-1} + c_n + \gamma_n^+ c_{n+1} = 0 \qquad -\infty < n < \infty \qquad . \qquad (A.35)$$

Define

$$u_n \equiv \frac{c_{n-1}}{c_n} \qquad v_n \equiv \frac{c_{n+1}}{c_n} \tag{A.36}$$

and divide (A.35) by c_n; then

$$\gamma_n^- u_n + 1 + \gamma_n^+ v_n = 0 \ . \tag{A.37}$$

Now divide (A.50) by c_{n-1} to obtain

$$\gamma_n^- + v_{n-1} + \gamma_n^+ (v_n/u_n) = 0 \tag{A.38}$$

Solve (A.37) for u_n and insert u_n into Eq. (A.38), obtaining

$$\gamma_n^- + v_{n-1} + \gamma_n^+ v_n \left(\frac{\gamma_n^-}{-1 - \gamma_n^+ v_n} \right) = 0 \ . \tag{A.39}$$

Solve Eq.(A.39) for v_{n-1} and shift the index up by one; then

$$v_n = - \frac{\gamma_{n+1}^-}{1 + \gamma_{n+1}^+ v_{n+1}} \ . \tag{A.40}$$

In continued fraction form, Eq. (A.40) is

$$v_n = - \frac{\gamma_{n+1}^-}{1^-} \frac{\gamma_{n+1}^+}{1^-} \frac{\gamma_{n+2}^-}{1^-} \frac{\gamma_{n+2}^+}{1^-} \frac{\gamma_{n+3}^-}{} \cdots \qquad -\infty < n < \infty \ . \tag{A.41}$$

where each minus sign in the denominator acts on everything to the right of it.

To find u_n, we divide Eq.(A.35) by c_{n+1} instead of c_{n-1}; the remaining steps are analagous. The result is

$$u_n = -\frac{\gamma^+_{n-1}}{1 + \gamma^-_{n-1}\, u_{n-1}} = -\frac{\gamma^+_{n-1}}{1^-}\,\frac{\gamma^-_{n-1}\,\gamma^+_{n-2}}{1^-}\,\frac{\gamma^-_{n-2}\,\gamma^+_{n-3}}{1^-}\cdots$$

$$-\infty < n < \infty \quad . \qquad \text{(A.42)}$$

Equations (A.41) and (A.42) are the desired Eqs. (87).

REFERENCES

1. C. V. Raman, Indian J. Phys. 2, 387 (1928).
2. C. V. Raman and U. S. Krishnan, Nature 121, 501 (1928).
3. P. A. Wolff, Proceedings 2nd International Conference on Light Scattering in Solids (Paris, 1971).
4. L. Brillouin, Ann. Phys. (Paris) 17, 88 (1922).
5. Y. R. Shen and N. Bloembergen, Phys. Rev. 137, 1787 (1965).
6. N. Bloembergen, Am. J. Phys. 35, 989 (1967).
7. N. M. Kroll, J. Appl. Phys. 36, 34 (1965).
8. W. H. Louisell, Coupled Mode and Parametric Electronics (Wiley, New York, 1960).
9. M. T. Raiford, Phys. Rev. A9, 2060 (1974).
10. K. Nishikawa, J. Phys. Soc. Japan 24, 916 (1968) and J. Phys. Soc. Japan 24, 1152 (1968).
11. V. P. Silin, Zh. Eksp. Teor. Fiz. 48, 1679 (1965) (Sov. Phys. JETP 21, 1127 (1965)).
12. L. M. Gorbunov, Zh. Eksp. Teor. Fiz. 55, 2298 (1969) (Sov. Phys. JETP 28, 1220 (1969)).
13. D. F. Dubois and M. V. Goldman, Phys. Rev. 164, 207 (1967).
14. J. R. Sanmartin, Phys. Fluids 13, 1533 (1970).
15. M. V. Goldman, Annals of Phys. (N.Y.) 38, 95 (1966).
16. E. A. Jackson, Phys. Rev. 153, 235 (1967).
17. N. Bloembergen and Y. R. Shen, Phys. Rev. 141, 29 (1966).
18. T. F. Volkov, Plasma Physics and the Problem of Controlled Thermonuclear Reactions (Pergamon Press, New York, 1958), Vol. 4.
19. G. G. Comisar, Phys. Rev. 141, 200 (1966).
20. V. Ts. Gurovich and V. I. Karpman, Sov. Phys. JETP 29, 1048 (1969).

21. S. E. Bodner and J. L. Eddleman, Phys. Rev. A5, 355 (1972).

22. I. S. Danilkin, Sov. Phys. Tech. Phys. 10, 524 (1965).

23. M. Porkolab, Parametric Instabilities and Enhanced Heating of Plasma in a Magnetic Field: A Review, MATT-1049, June 1974.

24. S. Bujarbarua, A. Sen, and P. Kaw, Phys. Letters 47A, 464 (1974).

25. R. L. Berger, M. V. Goldman, and D. F. Dubois, Phys. Fluids 18, 207 (1975).

26. J. A. Armstrong, N. Bloembergen, J. Ducuing, and P. S. Pershan, Phys. Rev. 127, 1918 (1962).

27. R. Z. Sagdeev and A. A. Galeev, Nonlinear Plasma Theory (W. A. Benjamin, Inc., New York, 1969), Chap. I.

28. H. Wilhelmsson, Physica Scripta 9, 61 (1974).

29. B. Cohen, A. N. Kaufman, and K. Watson, Phys. Rev. Lett. 29, 581 (1972).

30. A. N. Kaufman and B. Cohen, Phys. Rev. Lett. 30, 1306 (1973).

31. B. Cohen, Phys. Fluids 17, 496 (1974).

32. B. Cohen, M. Mostrom, D. Nicholson, A. Kaufman, C. Max, and A. B. Langdon, Phys. Fluids 18, 470 (1975).

33. Bruce I. Cohen, Ph.D. Thesis, 1975.

34. C. S. Liu, M. N. Rosenbluth, and R. B. White, Phys. Fluids 17, 1211 (1974).

35. K. J. Harker and F. W. Crawford, J. Geophys. Res. 75, 5459 (1970).

36. Yu. M. Aliev, O. M. Gradov, and A. Yu. Kirii, Sov. Phys. Tech. Phys. 17, 1453 (1973).

37. R. A. Cairns, J. Plasma Phys. 12, 169 (1974).

38. J. F. Drake and Y. C. Lee, Phys. Rev. Lett. 31, 1197 (1973).

39. D. F. DuBois, M. V. Goldman, and D. McKinnis, Phys. Fluids 16, 2257 (1973).

40. Y. C. Lee and P. K. Kaw, Phys. Rev. Lett. 32, 135 (1974).

41. C. Maroli, J. Plasma Phys. 10, 165 (1973).

42. F. W. Perkins and J. Flick, Phys. Fluids 14, 2012 (1971).

43. A. D. Piliya and V. I. Federov, Sov. Phys. Tech. Phys. 19, 686 (1974).

44. A. D. Piliya, Sov. Phys.-JETP 37, 629 (1973).

45. A. D. Piliya, JETP Letters 7, 266 (1973).

46. A. B. Shvartsburg, Sov. Phys. Dokl. 18, 654 (1974).

47. V. N. Tsytovich, L. Stenflo, H. Wilhelmsson, H.-G. Gustavsson, and K. Östberg, Physica Scripta 7, 241 (1973).

48. S. Wolschke, Beitrage Plasmaphysik 12, 273 (1972).

49. T. Amano and M. Okamoto, J. Phys. Soc. Japan 26, 529 (1969).

50. D. Forslund, J. Kindel, and E. Lindman, Phys. Rev. Lett. 30, 739 (1973).

51. A. A. Galeev, G. Laval, T. M. O'Neil, M. N. Rosenbluth, and R. Z. Sagdeev, JETP Letters 17, 35 (1973).

52. A. A. Galeev, G. Laval, T. M. O'Neil, M. N. Rosenbluth, and R. Z. Sagdeev, Sov. Phys.-JETP 38, 482 (1974).

53. M. N. Rosenbluth and R. Z. Sagdeev, Nuc. Fusion 13, 941 (1973).

54. R. B. White, C. S. Liu, and M. N. Rosenbluth, Phys. Rev. Lett. 31, 520 (1973).

55. D. Forslund and A. Galeev, Report of the Working Group on Stimulated Backscatter, IC/73/125, September 1973.

56. D. Pesme, G. Laval, and R. Pellat, Phys. Rev. Lett. 31, 203 (1973).

57. M. N. Rosenbluth, Phys. Rev. Lett. 29, 565 (1972).

58. A. D. Piliya, Proceedings 10th Conference on Phenomena in Ionized Gases, Oxford (1971).

59. D. F. DuBois and E. Williams, CU #1005 (1973).

60. M. N. Rosenbluth, R. B. White, and C. S. Liu, Phys. Rev. Lett. 31, 1190 (1973).

61. G. Laval, R. Pellat, and D. Pesme, Phys. Lett. 46A, 281 (1973).

62. A. N. Kaufman, private communication.

63. D. W. Forslund, J. M. Kindel, and E. L. Lindman, LA-UR-73-500 (1973).

64. R. White, P. Kaw, D. Pesme, M. N. Rosenbluth, G. Laval, R. Huff, and R. Varma, Nuclear Fusion 14, 45 (1974).

65. D. F. DuBois, D. W. Forslund, and E. A. Williams, Phys. Rev. Lett. 33, 1013 (1974).

66. F. Chambers and A. Bers (M.I. T.-R. L. E.), private communication, February 1975.

67. Dwight R. Nicholson and Allan N. Kaufman, Phys. Rev. Lett. 33, 1207 (1974).

68. M. N. Rosenbluth, R. B. White, and C. S. Liu, Phys. Rev. Lett. 31, 1190 (1973).

69. P. Kaw, R. White, D. Pesme, M. Rosenbluth, G. Laval, R. Varma, and R. Huff, Comments Plasma Phys. Controlled Fusion 2, 11 (1974).

70. C. S. Liu, M. N. Rosenbluth, and R. B. White, Phys. Rev. Lett. 31, 697 (1973).

71. M. Y. Yu, P. K. Shukla, and K. H. Spatschek, Temporally Growing Parametric Instability in a Turbulent, Inhomogeneous Plasma, preprint, 1975.

72. K. H. Spatschek, P. K. Shukla, and M. Y. Yu, Phys. Letters 51A, 183 (1975).

73. M. N. Rosenbluth and E. A. Williams in Proceedings of the Fifth Annual Anomalous Absorption Conference, Los Angeles, April 1975.

74. R. Pellat, D. Pesme, G. Laval in Proceedings of the Fifth Annual Anomalous Absorption Conference, Los Angeles, April 1975.

75. S. S. Jha and S. Srivastava, Phys. Rev. A11, 378 (1975).

76. Proceedings of the Fifth Annual Anomalous Absorption Conference, Los Angeles, 1975.

77. A. N. Kaufman (Univ. of California, Berkeley), private communication, May, 1973.

78. R. Briggs, Electron Stream Interaction With Plasma, MIT Press (1964).

79. B. D. Fried, G. Schmidt, and R. W. Gould, Proceedings Sixth European Conference on Controlled Fusion and Plasma Physics, page 477 (1972).

80. E. S. Cassedy and C. R. Evans, J. Appl. Phys. 43, 4452 (1972).

81. D. L. Bobroff and H. A. Haus, J. Appl. Phys. 38, 390 (1967).

82. N. M. Kroll and P. L. Kelley, Phys. Rev. A4, 763 (1971).

83. J. D. Bjorken and S. D. Drell, Relativistic Quantum Fields (McGraw-Hill, New York, 1965).

84. C. S. Liu and K. Nishikawa, preprint, 1974.

85. L. M. Gorbunov, Sov. Phys. JETP 35, 1119 (1972).

86. J. Heading, An Introduction to Phase-Integral Methods (Wiley, New York, 1962).

87. R. N. Sudan, Phys. Fluids 8, 1899 (1965).

88. D. W. Forslund, J. M. Kindel, and E. L. Lindman, private communication.

89. R. L. Carmen, F. Shimizu, C. S. Wang, and N. Bloembergen, Phys. Rev. A2, 60 (1970).

90. S. E. Bodner, UCRL Report No. UCRL-74074, 1972.

91. S. Tamor, Phys. Fluids 16, 1169 (1973).

92. E. J. Valeo and C. R. Oberman, Phys. Rev. Lett. 30, 1035 (1973).

93. J. J. Thomson, W. L. Kruer, S. E. Bodner, and J. S. DeGroot, Phys. Fluids 17, 849 (1974).

94. J. J. Thomson and J. I. Karush, Phys. Fluids 17, 1608 (1974).

95. J. J. Thomson, Finite Bandwidth Effects on the Parametric Instability in an Inhomogeneous Plasma, UCRL-79538, August 1974.

96. V. V. Tamoikin and S. M. Fainshtein, Sov. Phys. JETP 35, 115 (1972).

97. J. L. Emmett, J. Nuckolls, and L. Wood, Sci. Amer. 230, No. 6, 24 (1974).

98. K. A. Brueckner and S. Jorna, Rev. Mod. Phys. 46, 325 (1974).

99. P. Mulser, R. Sigel, and S. Witkowsky, Phys. Letters 6C, 187 (1973)

100. J. S. Clark, H. N. Fisher, and R. J. Mason, Phys. Rev. Lett. 30, 89 (1973).

101. J. Nuckolls, L. Wood, A. Thiessen, and G. Zimmerman, Nature 239, 139 (1972).

102. J. Drake, P. Kaw, Y. C. Lee, G. Schmidt, C. S. Liu, and M. N. Rosenbluth, Phys. Fluids 17, 778 (1974).

103. James R. Albritton, Phys. Fluids 18, 51 (1975); A. V. Vinogradov, B. Ya. Zel'dovich, and I. I. Sobel'man, JETP Letters 17, 271 (1973).

104. Laser Interaction and Related Plasma Phenomena, edited by H. Hora and H. J. Schwartz (Plenum, New York, 1974), Vol. 3.

105. J. L. Bobin, M. Decroisette, B. Meyer, and Y. Vitel, Phys. Rev. Lett. 30, 594 (1973).

106. J. Soures, L. M. Goldman, and M. Lubin, Nuclear Fusion 13, 829 (1973).

107. D. W. Forslund, J. M. Kindel, and E. L. Lindman, Phys. Rev. Lett. 30, 739 (1973).

108. W. L. Kruer, K. G. Estabrook, and K. H. Sinz, Nuclear Fusion 13, 952 (1973).

109. J. Martineau and J.-L. Bobin, Phys. Letters 47A, 43 (1974).

110. C. S. Liu, preprint, 1974.

111. P. L. Mascheroni, Phys.Rev. Lett. 34, 141 (1975).

112. A. Bers, F. W. Chambers, and D. C. Watson, in Proceedings of the Fourth Annual Anomalous Absorption Conference, Livermore, 1974.

113. A. B. Langdon, B. F. Lasinski, and W. L. Kruer, Plasma Heating at One-Quarter Critical Density, UCRL-75018, August 1973.

114. Michael A. Mostrom, Ph.D. Thesis, 1975.

115. H. E. Klein, W. M. Manheimer, and E. Ott, Phys. Rev. Lett. 31, 1187 (1973).

116. C. S. Liu, M. N. Rosenbluth, and R. White, Proceedings of the Fifth Conference on Plasma Physics and Controlled Nuclear Fusion Research, Tokyo, 1974.

117. M. A. Mostrom, D. R. Nicholson, and A. N. Kaufman, Nonlinear Attentuation of an Electromagentic Beam by Side- and Back-scattering in an Inhomogeneous Plasma, LBL-2032, May 1973.

118. D. Biskamp and H. Welter, Phys. Rev. Lett. 34, 312 (1975).

119. F. M. Arscott, Periodic Differential Equations (Pergamon Press, Oxford, 1964).

120. W.Magnus and S. Winkler, Hill's Equations (Interscience Publishers, New York, 1966).

121. L. Brillouin, Wave Propagation in Periodic Structures (McGraw-Hill, New York, 1946).

122. W. Magnus, F. Oberhettinger, and R. P. Soni, Formulas and Theorems for the Special Functions of Mathematical Physics (Springer-Verlag, New York, 1966).

123. Modern Computing Methods, National Physical Laboratory Notes on Applied Science No. 16 (Her Majesty's Stationery Office, London, 1961), Chapter 11.

FIGURE CAPTIONS

Fig. 1. The space-time response of Eqs. (25) in an infinite, homogeneous medium, with the initial conditons $a_1(X,T = 0) = \delta(X)$, $a_2(X,T = 0) = 0$. ($D_1 = D_2 = 0$, $V_2/V_1 = -1$). From Bobroff and Haus[81].

Fig. 2. The configuration for the finite pump extent, homogeneous medium case. Boundary conditions: If $V_j > 0$, $a_j(X = 0,T) = 0$; if $V_j < 0$, $a_j(X = L/L_o,T) = 0$; $i = 1,2$.

Fig. 3. Graphical olution of Eq. (34) for the temporal growth rate in the finite pump extent, homogeneous medium case. ($L/L_o = 9\pi/2$). From Bobroff and Haus[81].

Fig. 4. The space-time response of the finite pump, homogeneous medium case, to the initial conditions $a_1(X,T = 0) = \delta(X)$, $a_2(X,T = 0) = 0$. ($L/L_o = 2$, $V_2/V_1 = -1$, $D_1 = D_2 = 0$). From Bobroff and Haus[81].

Fig. 5. Analytic pulse response of the infinite pump extent, inhomogeneous plasma case, Eqs. (46) with $\kappa(X) = \kappa'X$, for the initial conditions $a_1(X,T = 0) = 0$, $a_2(X,T = 0) = \delta(X)$. ($\kappa' = 1.25$, $V_2/V_1 = -0.2$). From Rosenbluth, White, and Liu[60].

Fig. 6. Pulse response of the infinite, inhomogeneous system, Eqs. (46) with $\kappa(X) = \kappa'X$, by direct numerical integration, with the initial conditions $a_1(X,T = 0) = 0$, $a_2(X,T = 0) = \delta(X)$. ($\kappa' = 1.25$, $V_2/V_1 = -0.2$; compare Fig. 5).

Fig. 7. Wavenumber mismatch $\kappa(X) = 10 \tanh(X/10)$; and space-time response of Eqs. (46) with initial conditons $a_1(X,T = 0) = \delta(X)$, $a_2(X,T = 0) = 0$. ($V_2/V_1 = -1$).

Fig. 8. Wavenumber mismatch $\kappa(X) = \kappa' X$ and spatial pump variation $\gamma_o(X)$ for the case of finite pump extent, inhomogeneous plasma. The equations are solved with the initial conditions $a_1(X, T = 0) = \delta(X)$, $a_2(X, T = 0) = 0$, and the boundary conditions $a_1(X = 0, T) = 0$, $a_2(X = L/L_o, T) = 0$.

Fig. 9. Real and imaginary parts of the complex eigenfrequency for the case of finite pump extent, inhomogeneous plasma $\kappa(X) = \kappa' X$. The solid lines are from Forslund, Kindel, and Lindman[63]; the points are measured from our numerical integration of Eqs. (42). ($V_1 = 24$, $V_2 = -1$, $\nu_1 = \nu_2 = 0$, $\gamma_o = 24$, $\bar{L} = 5$). See Fig. 8 for configuration.

Fig. 10. $a_1(X, T)$ vs X for $0.25 \lesssim T \lesssim 4.25$, obtained by numerical integration of Eqs. (42). The parameters are those of Fig. 9, with $\kappa' = 1$. ($V_1 = 24$, $V_2 = -1$, $\nu_1 = \nu_2 = 0$, $\gamma_o = 24$, $\bar{L} = 5$). See Fig. 8 for configuration.

Fig. 11. Complex growth rate $\gamma + i\Omega$ vs length $\bar{L}$ of finite pump. From Forslund, Kindel, and Lindman[63]. ($\kappa' = 0.4$, $V_1 = 24$, $V_2 = -1$, $\nu_1 = \nu_2 = 0$, $\gamma_o = \sqrt{24}$). See Fig. 8 for configuration.

Fig. 12. Amplification $A \equiv |a_1(X = L/L_o, T)|/a_o$, where a_o a $a_o \equiv a_1(X = 0, T)$ is the constant input, vs inhomogeneity κ'. From numerical integration of Eqs. (46) with $\kappa(X) = \kappa' X$. ($V_2/V_1 = -1$, $L/L_o = 1$).

Fig. 13. The function $L_o^2 \, d\bar{\kappa}(x)/dx$ vs x/L_o at the threshold value $\Delta/L_o^{-1} = 0.1$ in Fig. 15. ($L_T/L_o = 1.27$ $V_2/V_1 = -1$, $\lambda^{-1} \equiv \bar{\kappa}' L_o^2 = 1$, $L/L_o = 400$; a particular realization of the set $\{\alpha_j\}$ is used.)

Fig. 14. The temporal evolution of $|a_2(x,t)|$ vs x/L_o for the initial conditions $a_1(x,t=0) = \delta(x)$, $a_2(x,t=0) = 0$. ($\Delta/L_o^{-1} = 0.5$, otherwise as in Fig. 13)

Fig. 15. The absolute growth rate γ/γ_o vs the RMS mismatch function Δ/L_o^{-1} (parameters as in Fig. 13).

Fig. 16. The absolute growth rate γ/γ_o vs the correlation length L_T/L_o (parameters as in Fig. 13).

Fig. 17. A schematic diagram of Raman backscattering in laser fusion geometry.

Fig. 18. Absolute growth rate γ/γ_o vs turbulent density fluctuation level Δ_n for the laser fusion situation of Section II-B. ($V_2/V_1 = -0.03$, $\bar{K}'L_o^2 = 0.67$, $L_T/L_o = 1.3$; a particular realization of the set $\{a_j\}$ was used.)

Fig. 19. Spatial growth rate vs modulation amplitude. ($V_2/V_1 = 1$). For each root k shown, $k + in$ is also a root, $-\infty < n < \infty$. The roots shown are purely real. $\kappa(X) = L_o\kappa_m \sin(XL_o/L_m)$.

Fig. 20. Spatial growth rate vs modulation amplitude. ($V_2/V_1 = 1$). For each root k shown, $k + in$ is also a root, $-\infty < n < \infty$. The roots shows are purely real. $\kappa(X) = L_o\kappa_m \sin(XL_o/L_m)$.

Fig. 21. Temporal growth rate vs modulation amplitude. ($V_2/V_1 = 1$). The roots which have solid lines in the $\mathrm{Im}(\omega)$ graph have zero real frequency. There are four roots corresponding to the four possible combinations of dashed lines in the $\mathrm{Re}(\omega)$ and in the $\mathrm{Im}(\omega)$ graph. The lots are growth rates of a pulse response to the initial conditions

$a_1(X,T = 0) = \delta(X)$, $a_2(X,T = 0) = 0$.

$\kappa(X) = L_o\kappa_m \sin(XL_o/L_m)$.

Fig. 22. Temporal growth rate vs modulation amplitude.

$(V_2/V_1 = -1, \quad \kappa' = 1)$. $\kappa(X) = \kappa'X + L_o\kappa_m \sin(XL_o/L_m)$.

Fig. 23. Temporal growth rate vs modulation amplitude.

$(V_2/V_1 = -1, \quad \kappa' = 1)$. $\kappa(X) = \kappa'X + L_o\kappa_m \sin(XL_o/L_m)$.

Fig. 24. Temporal growth rate vs modulation wavelength.

$(V_2/V_1 = -1, \quad \kappa' = 1)$. $\kappa(X) = \kappa'X + L_o\kappa_m \sin(XL_o/L_m)$.

Fig. 25. Absolute growth rate γ/γ_o vs modulation wavelength L_m/L_o and modulation amplitude $L_o\kappa_m$, combining the results of Figs. 22, 23, and 24. The dashed curve is a schematic curve representing the threshold curve in the L_m-κ_m plane.

$(V_2/V_1 = -1, \quad \kappa' = 1)$. $\kappa(X) = \kappa'X + L_o\kappa_m \sin(XL_o/L_m)$.

Fig. 26. Space-time response to the initial conditions

$a_1(X,T = 0) = \delta(X)$, $a_2(X,T = 0) = 0$.

$\kappa(X) = \kappa'X + L_o\kappa_m \sin(XL_o/L_m)$. $(L_o\kappa_m = 2, \quad L_m/L_o = 0.16,$

$V_2/V_1 = -1, \quad \kappa' = 1)$.

Fig. 27. The method of characteristics, discussed in Appendix D.

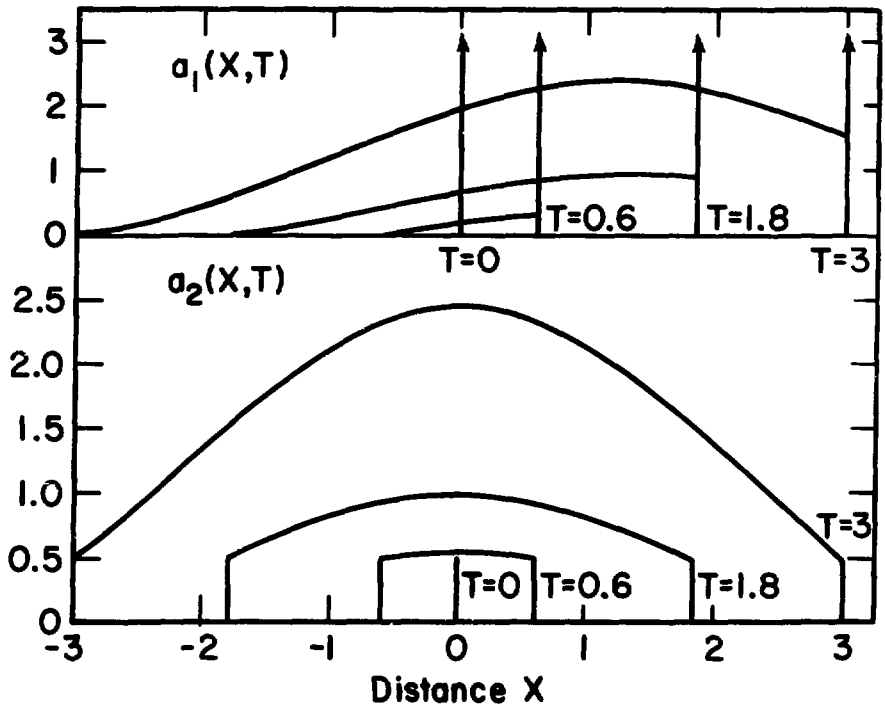

Fig. 1

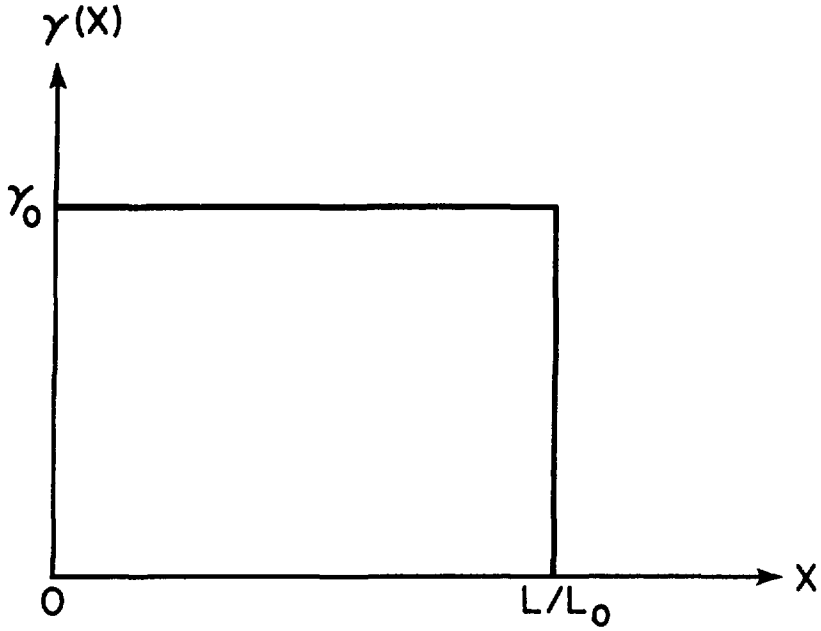

XBL757-3369

Fig. 2

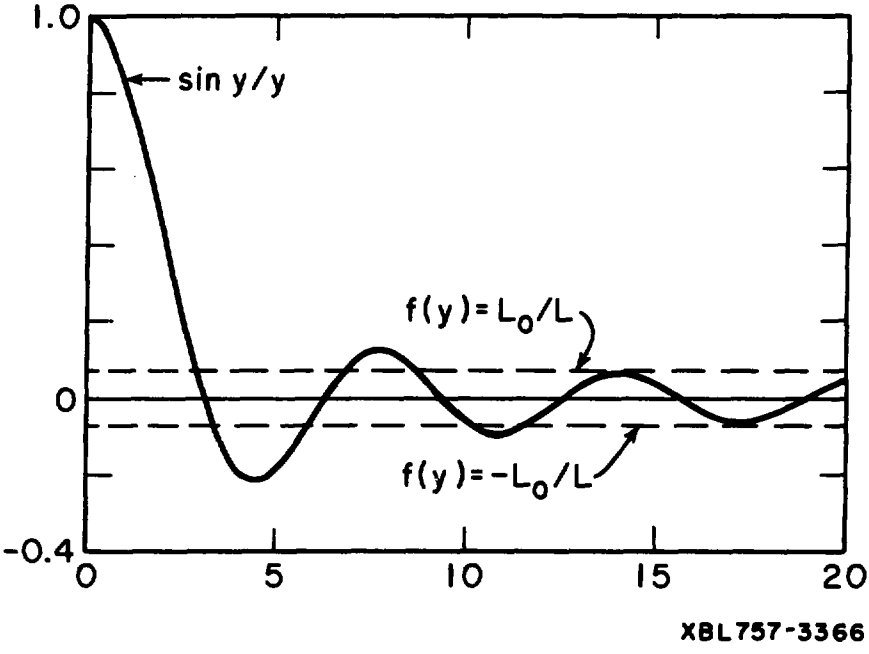

Fig. 3

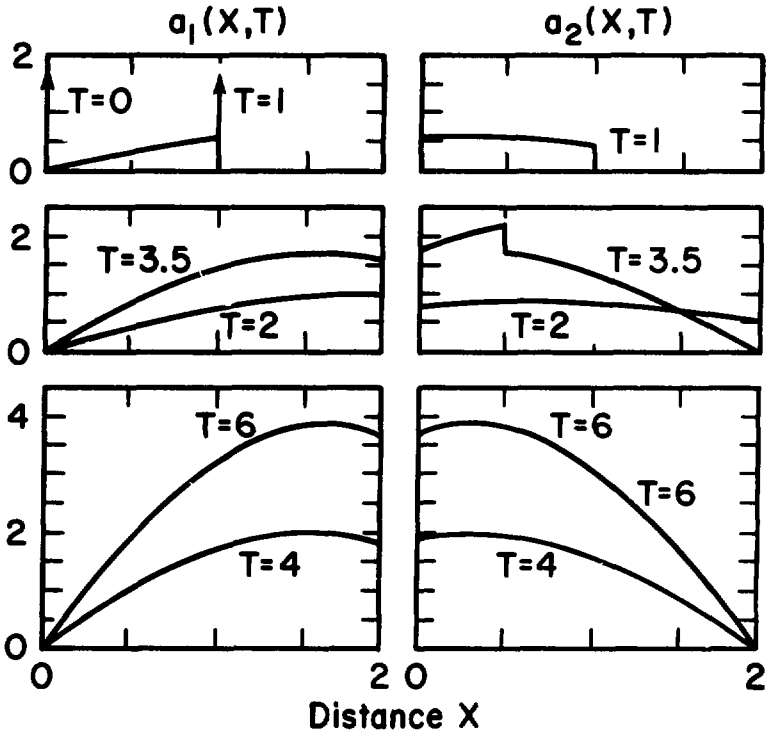

XBL757-3363

Fig. 4

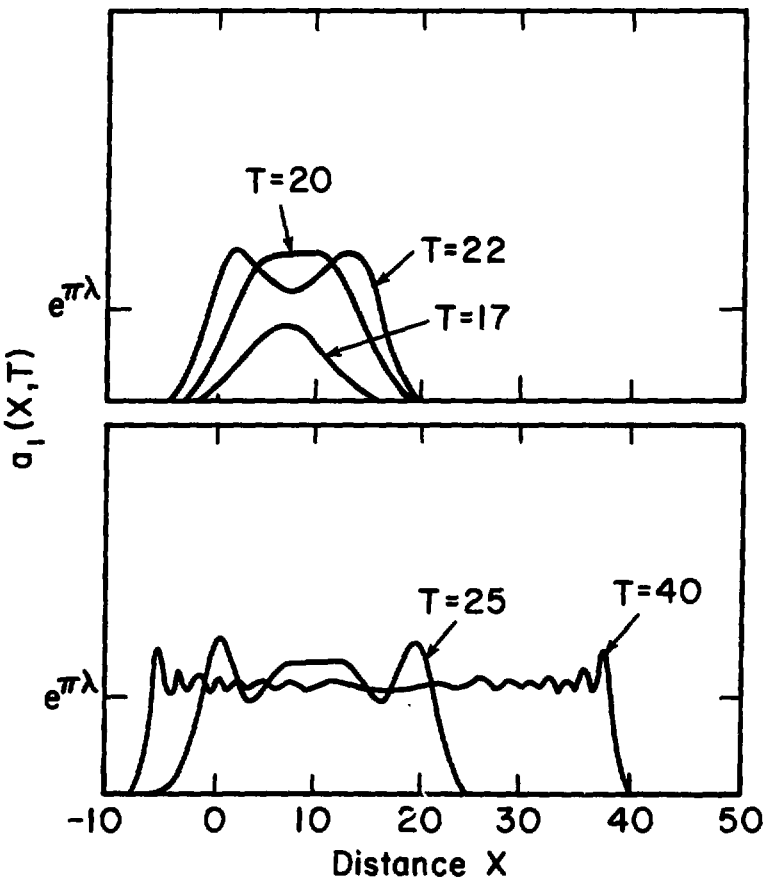

XBL 757-3362

Fig. 5

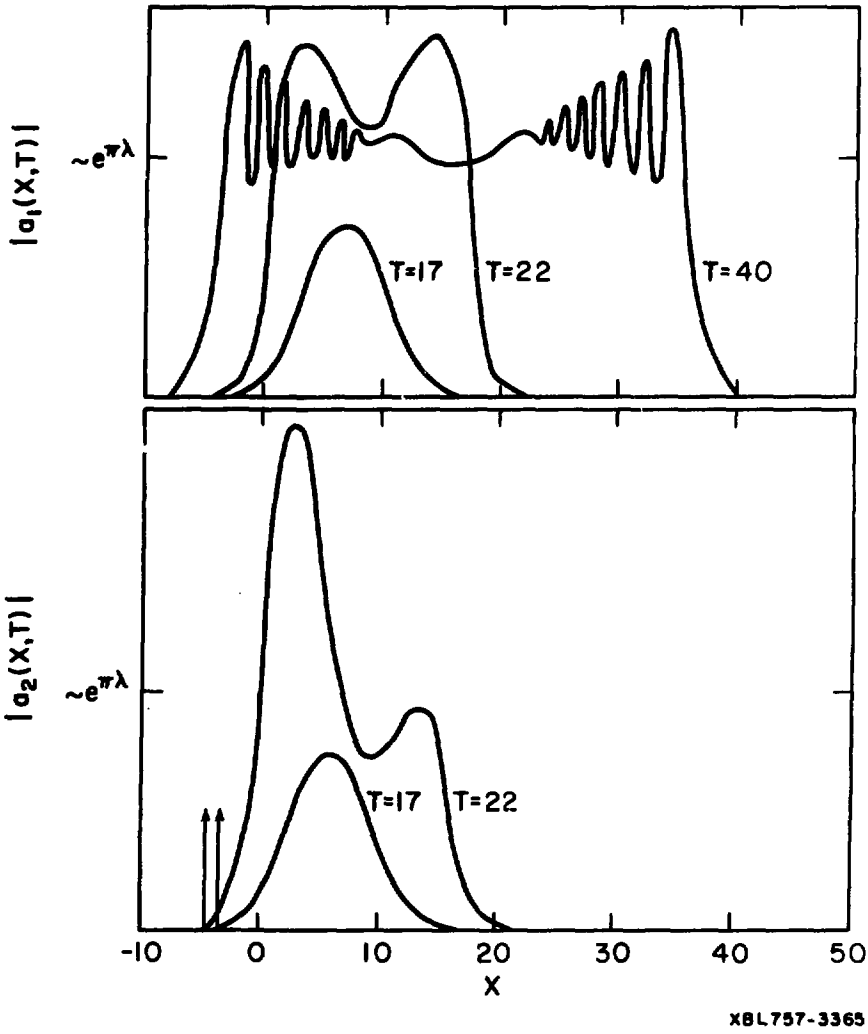
$|a_1(X,T)|$
$\sim e^{\pi\lambda}$
T=17
T=22
T=40
$|a_2(X,T)|$
$\sim e^{\pi\lambda}$
T=17
T=22
-10
0
10
20
30
40
50
X
XBL757-3365

Fig. 6

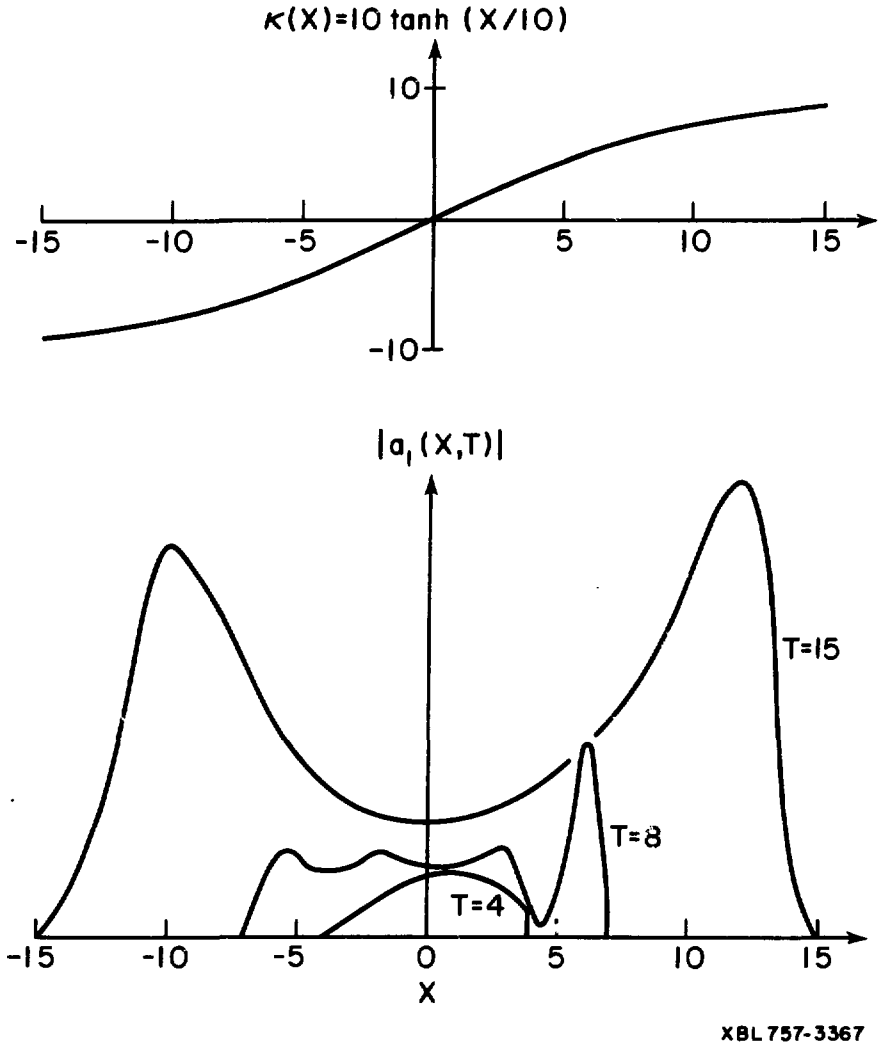
κ(X)=10 tanh (X/10)
10
-10
-15
-10
-5
5
10
15
|a1(X,T)|
T=15
T=8
T=4
-15
-10
-5
0
5
10
15
X
XBL 757-3367

Fig. 7

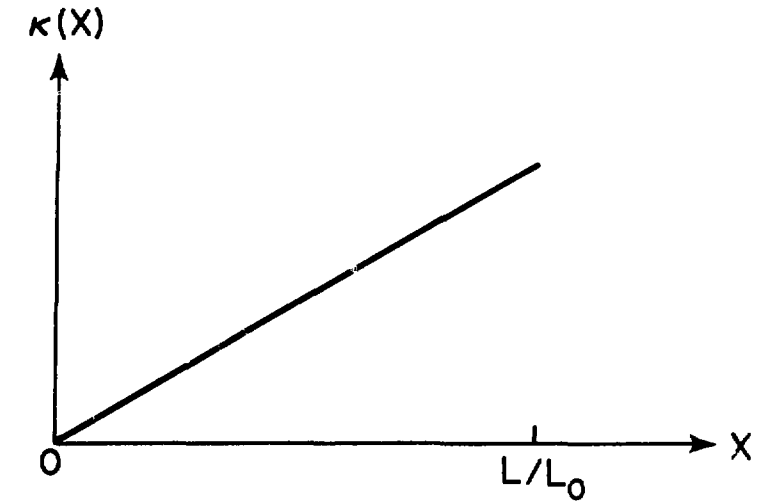

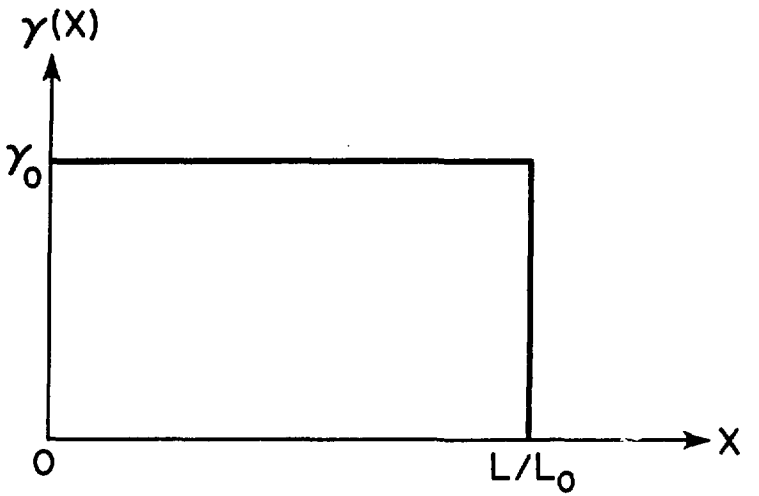

XBL757-3370

Fig. 8

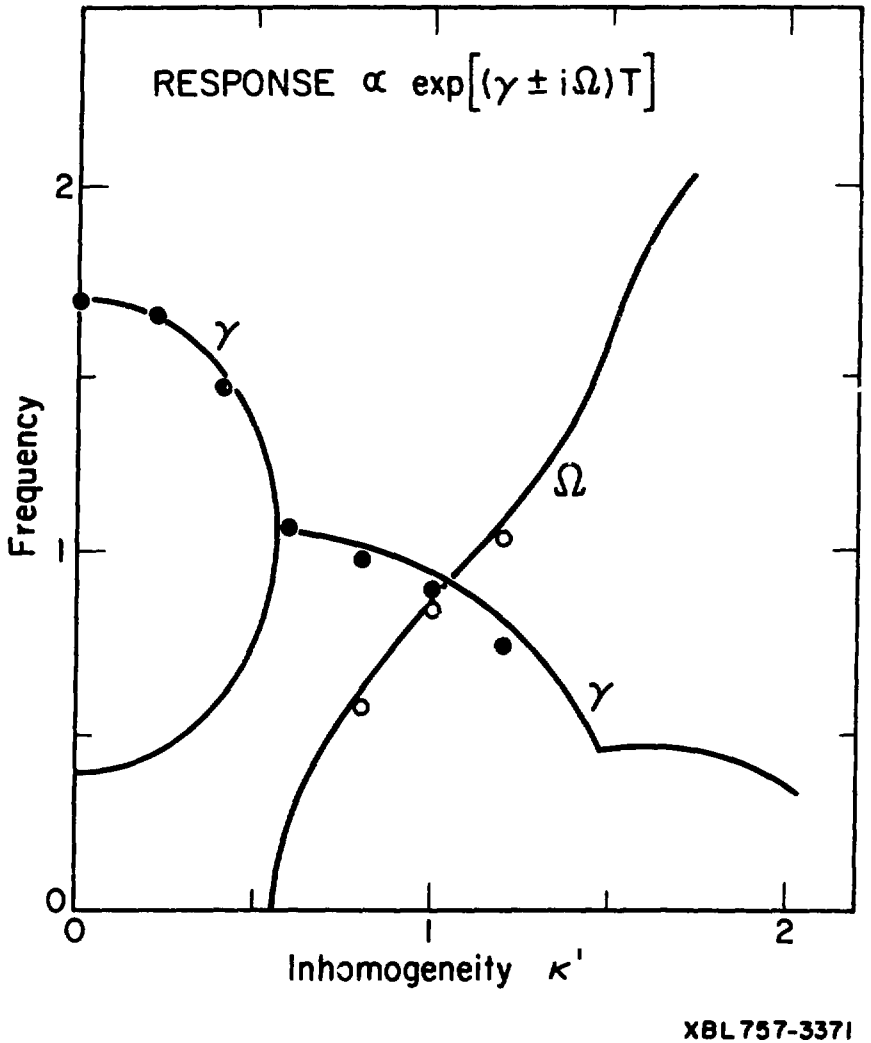
RESPONSE ∝ exp[(γ ± iΩ)T]
Frequency
Inhomogeneity κ'
γ
Ω
γ
0
1
2
0
1
2
XBL757-3371

Fig. 9

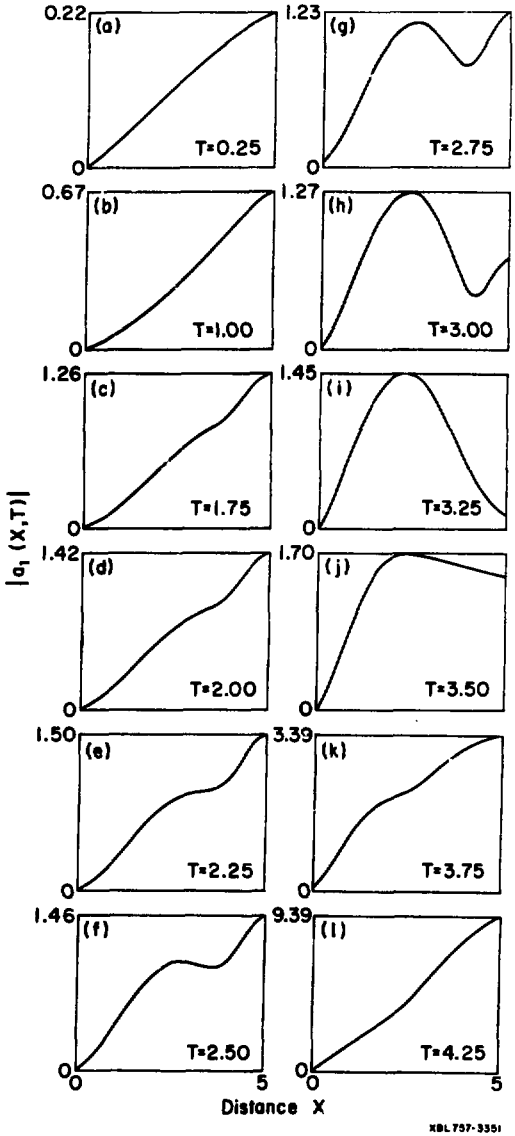
0.22
(a)
T=0.25
0
1.23
(g)
T=2.75
0
0.67
(b)
T=1.00
0
1.27
(h)
T=3.00
0
1.26
(c)
T=1.75
0
1.45
(i)
T=3.25
0
1.42
(d)
T=2.00
0
1.70
(j)
T=3.50
0
1.50
(e)
T=2.25
0
3.39
(k)
T=3.75
0
1.46
(f)
T=2.50
0
9.39
(l)
T=4.25
0
0
5
0
5
|a1 (X,T)|
Distance X
XBL 757-3351

Fig. 10

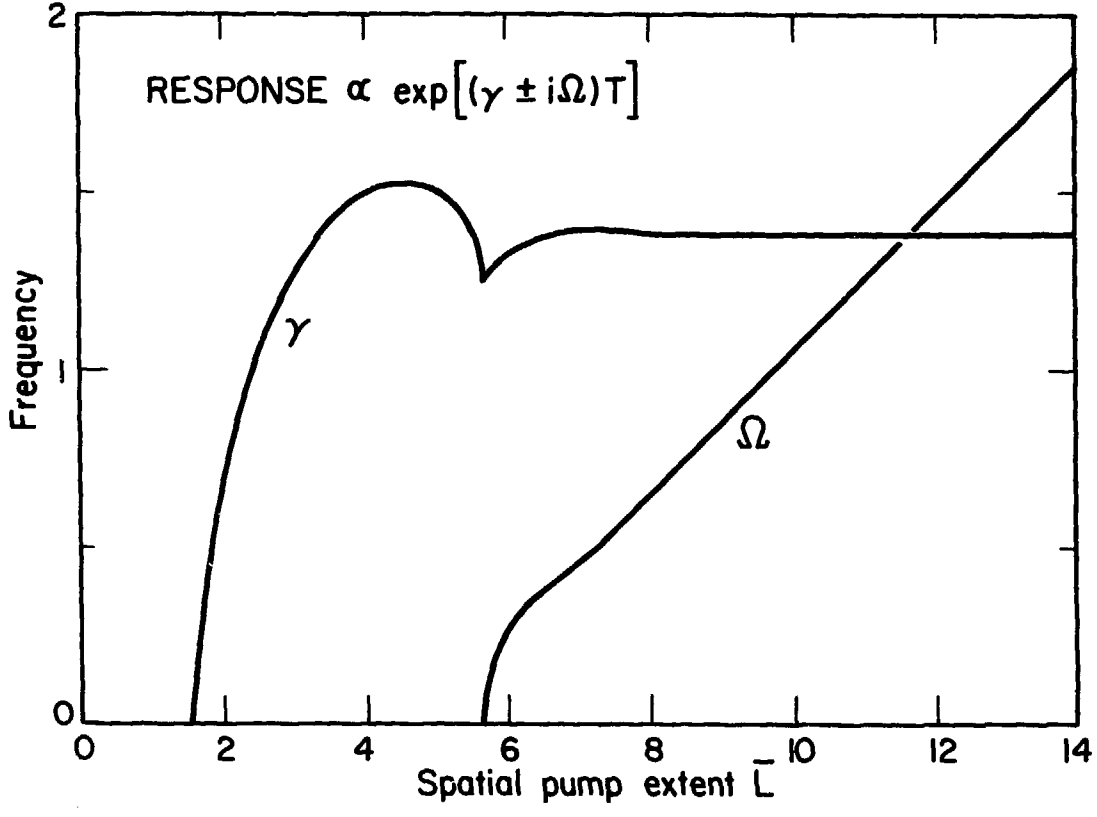

Fig. 11

XBL 757-3372

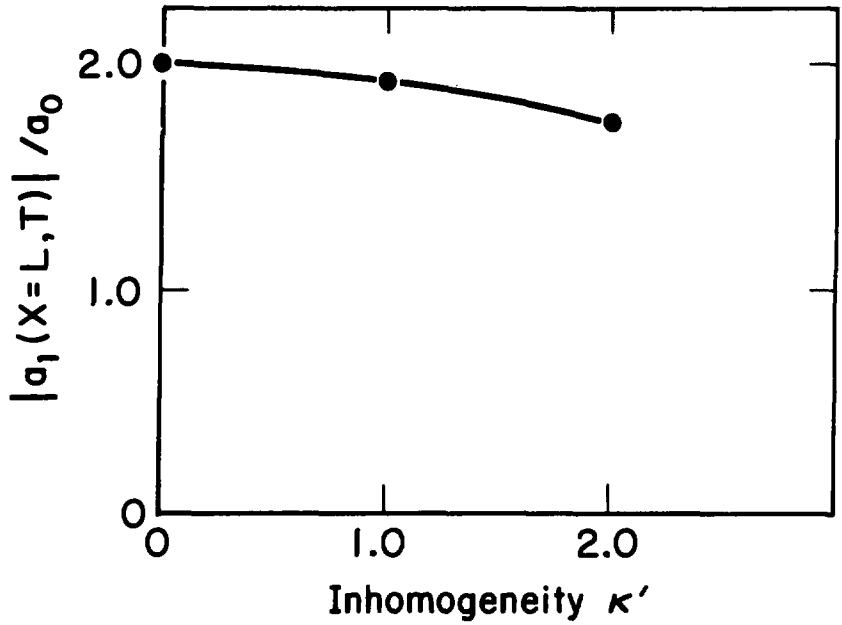

XBL757-3368

Fig. 12

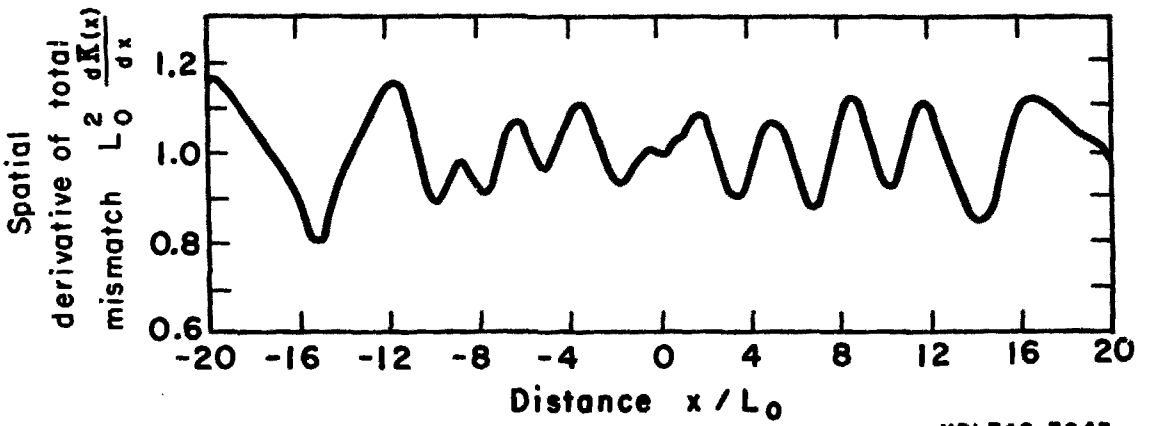
Spatial derivative of total mismatch $L_0^2 \frac{dK(x)}{dx}$
1.2
1.0
0.8
0.6
-20
-16
-12
-8
-4
0
4
8
12
16
20
Distance x / L_0
XBL748-3843

Fig. 13

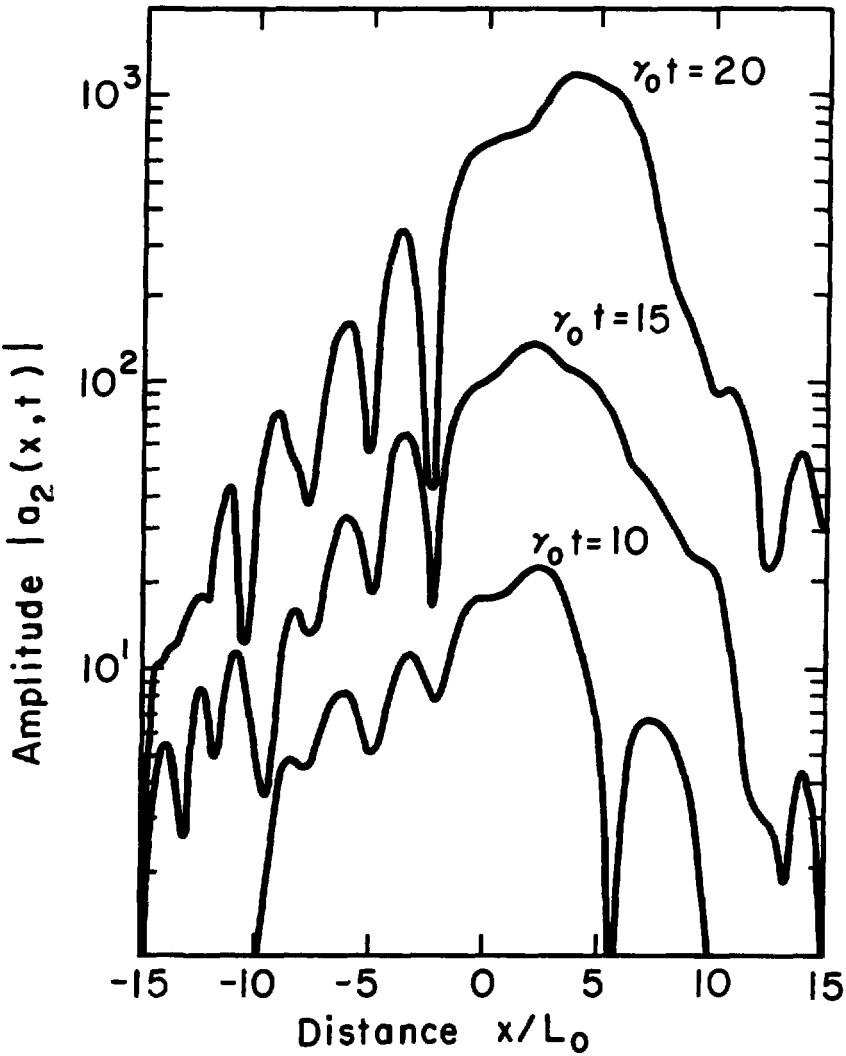

XBL748-3841

Fig. 14

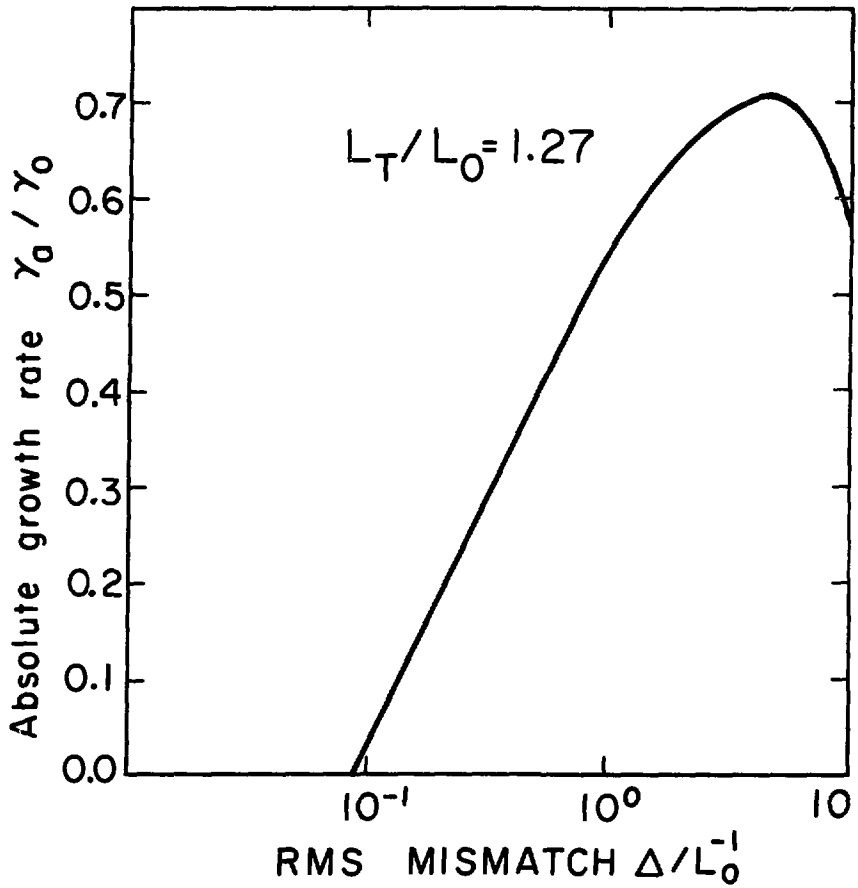

Fig. 15 XBL748-3844

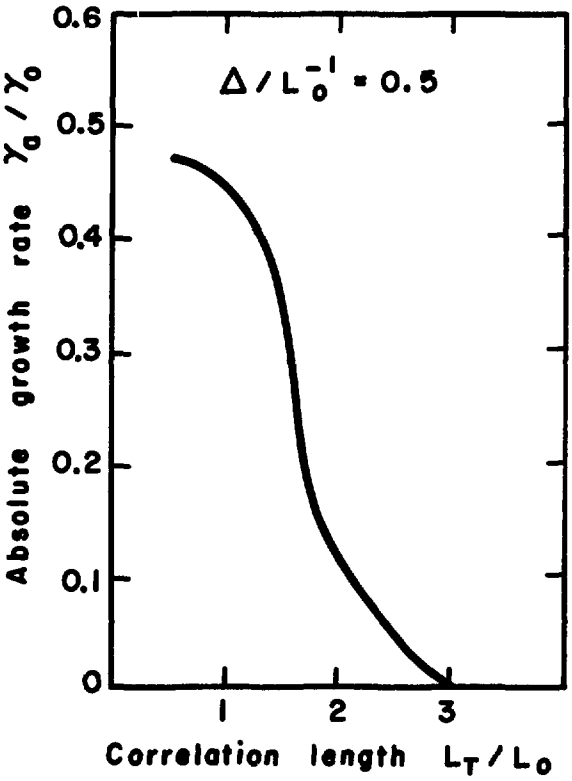

XBL 748 - 3842

Fig. 16

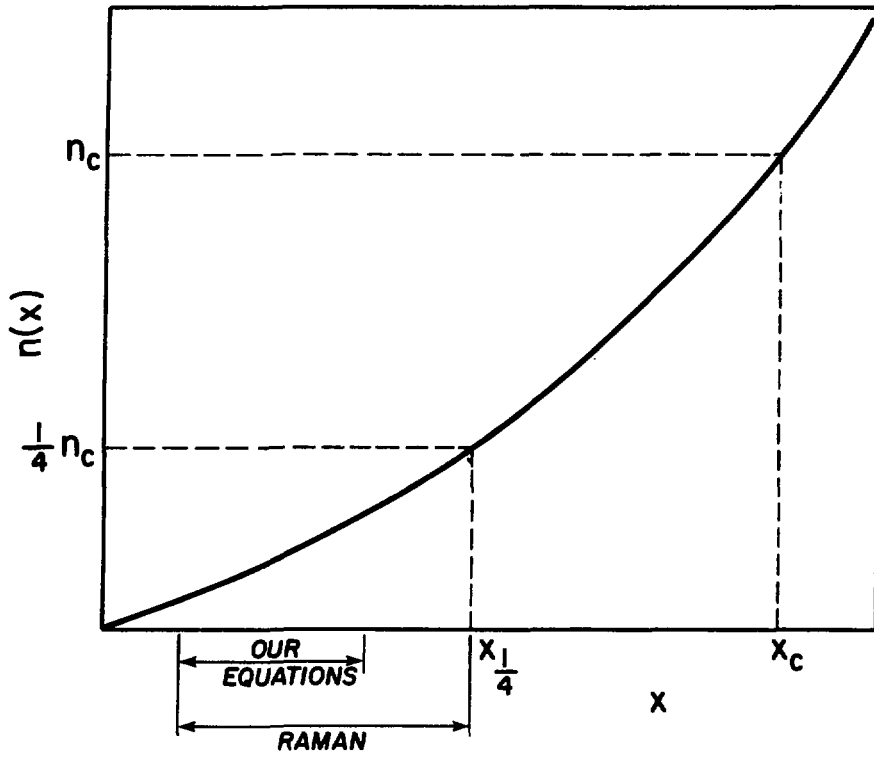

$$\omega_0 = \omega_1 + \omega_2$$
$$k_0 = |k_1| + k_2$$

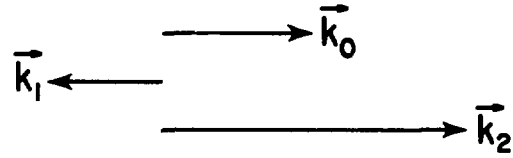

XBL757-3373

Fig. 17

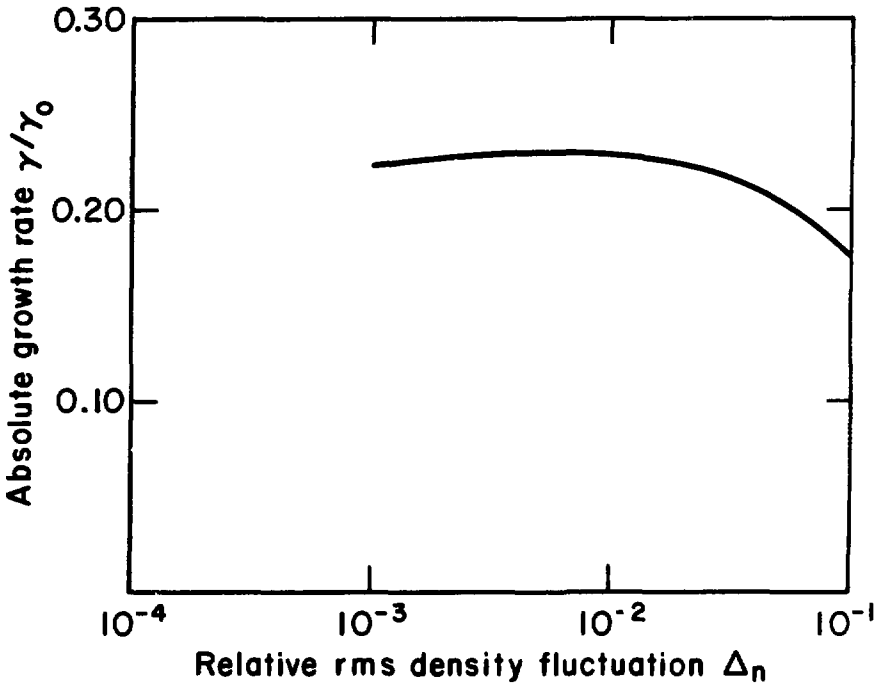

XBL 757-3360

Fig. 18

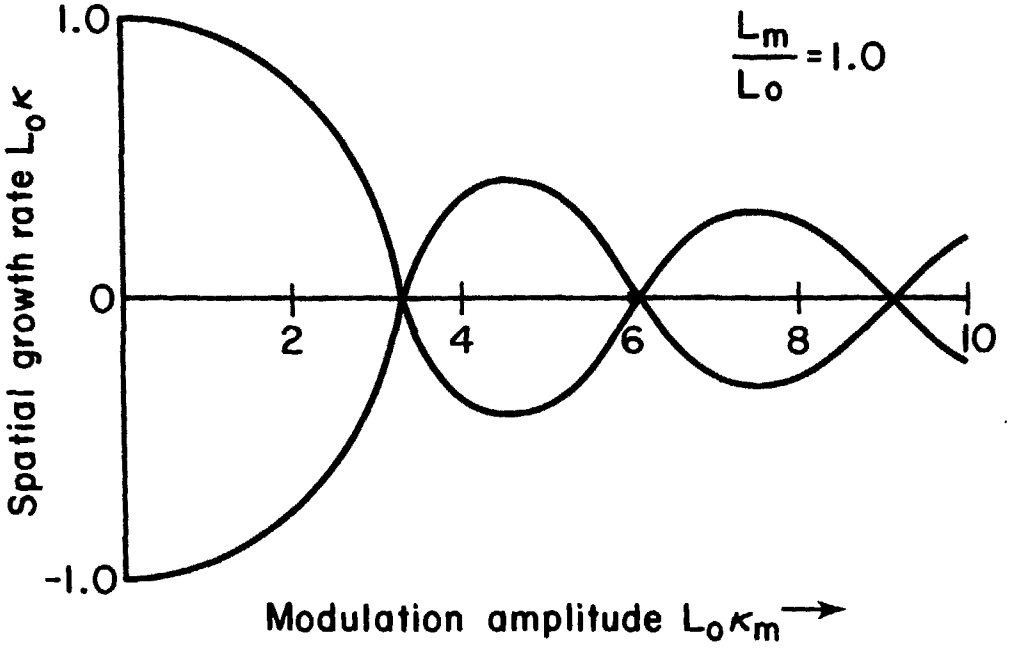

Fig. 19

XBL757-3357

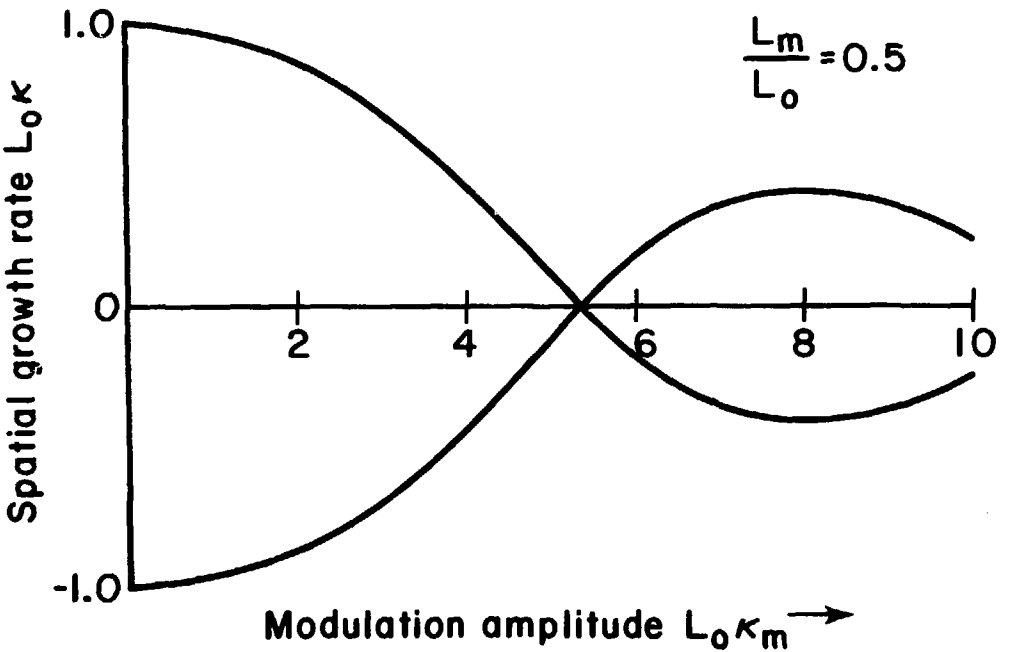
1.0
0
-1.0
Spatial growth rate $L_o\kappa$
$\frac{L_m}{L_o} = 0.5$
2
4
6
8
10
Modulation amplitude $L_o\kappa_m$
XBL 757-3358

Fig. 20

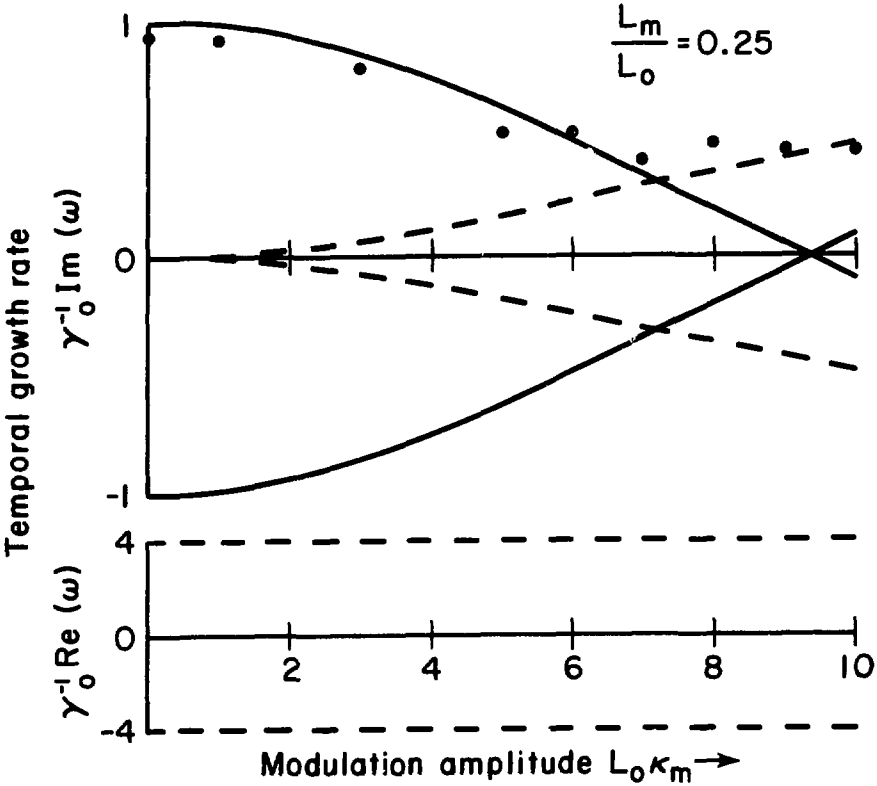

XBL 757-3359

Fig. 21

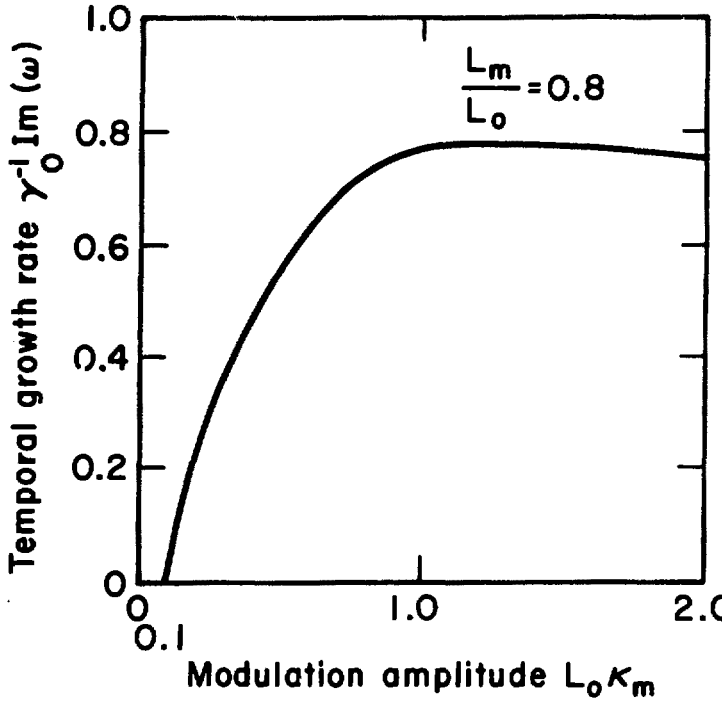

XBL 757-3355

Fig. 22

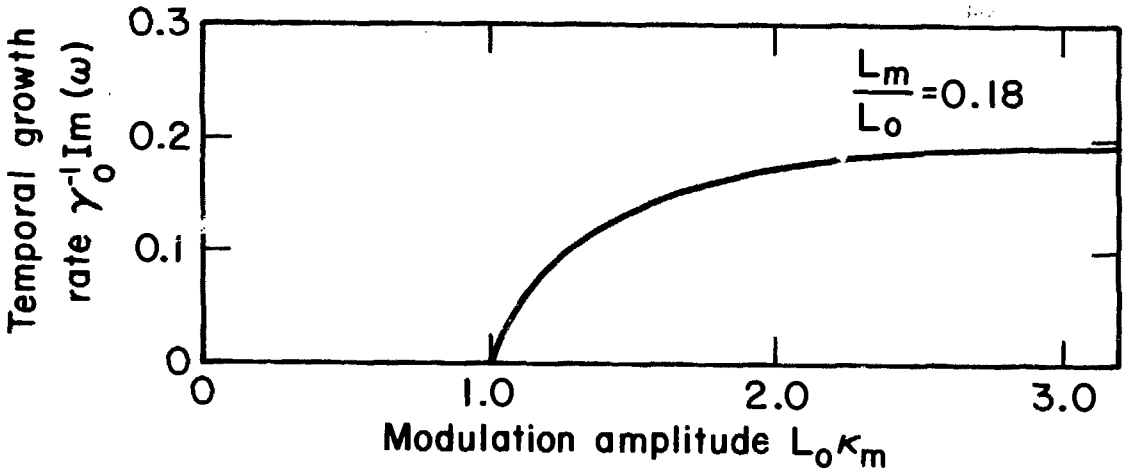

Fig. 23

XBL757-3356

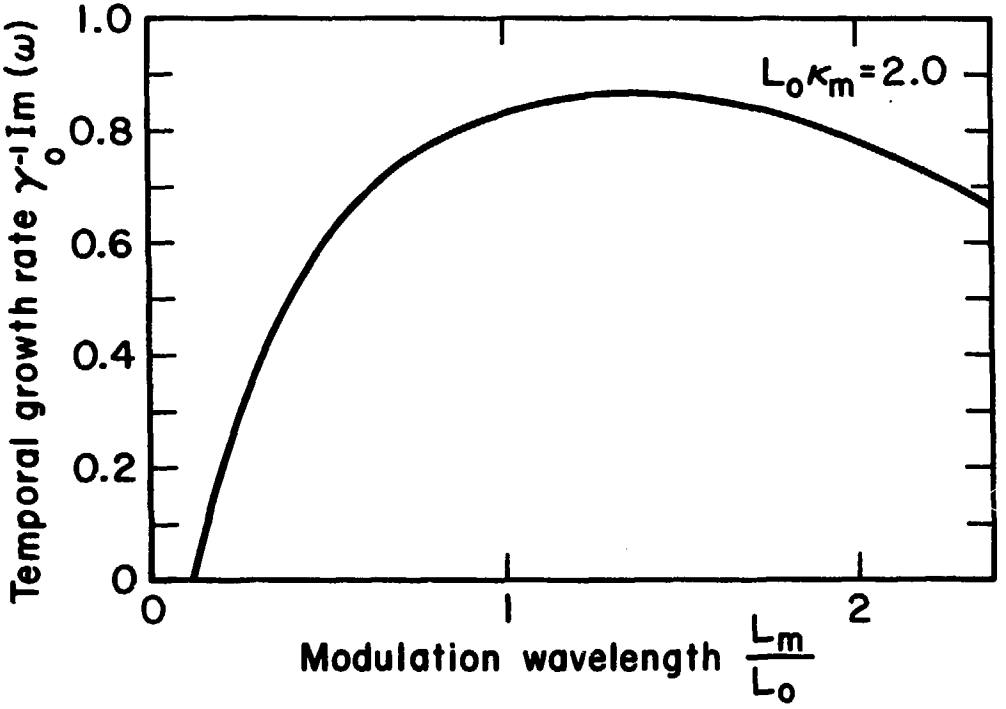

Fig. 24

XBL757-3354

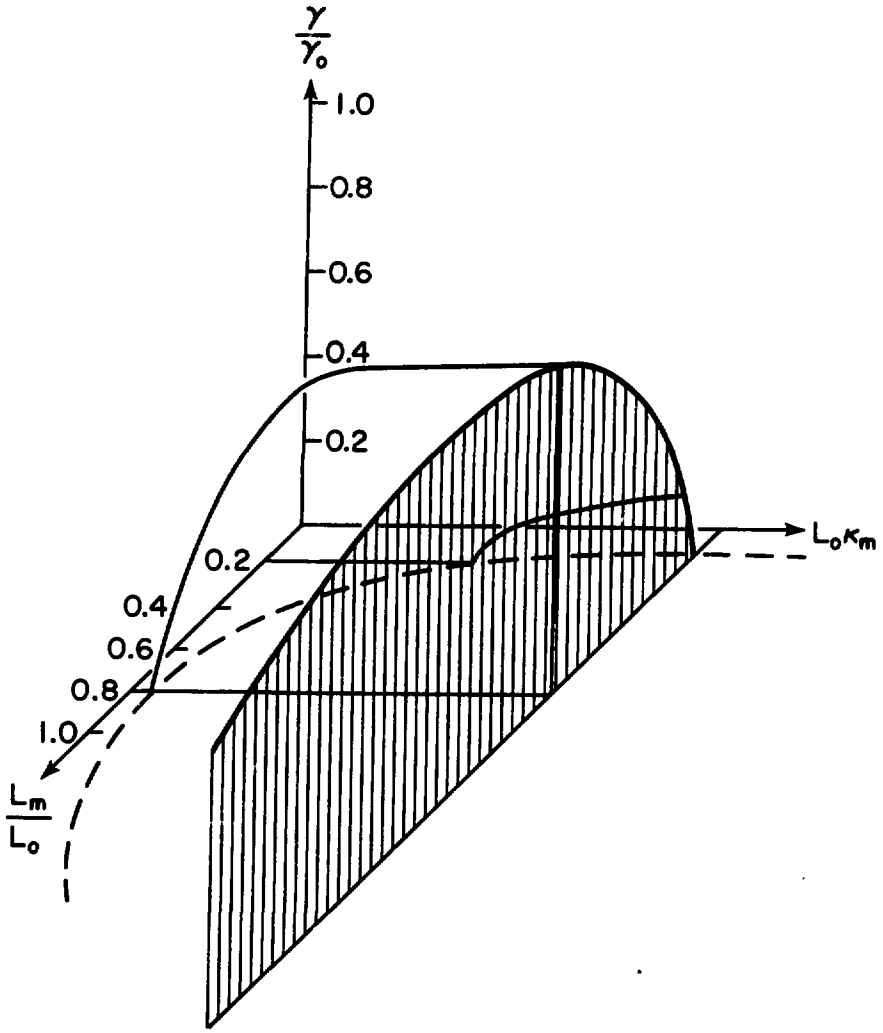

XBL 757-3352

Fig. 25

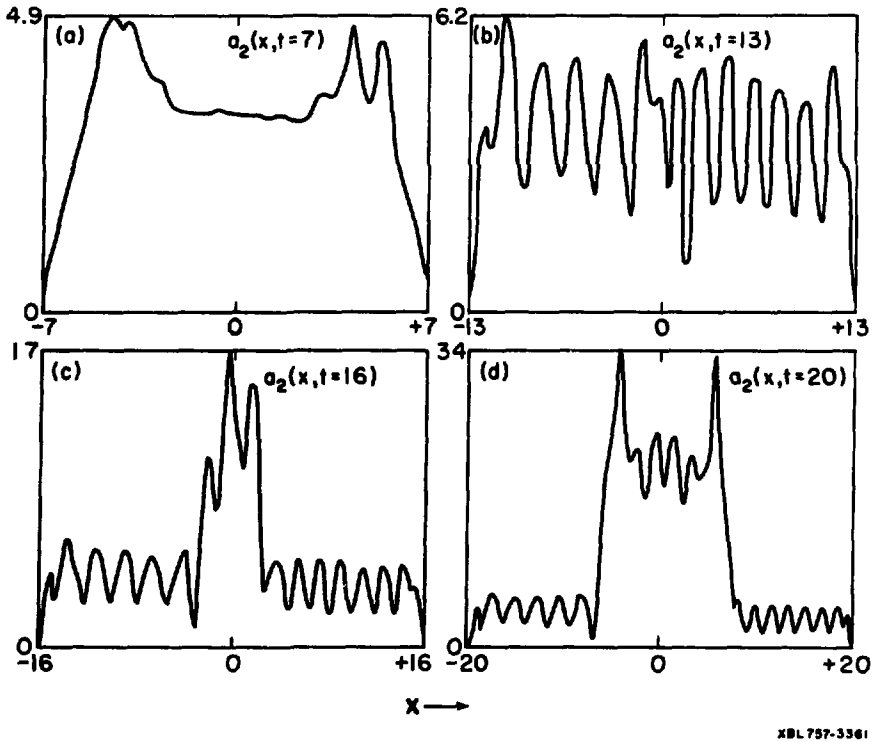
4.9
(a)
$a_2(x,t=7)$
0
-7
0
+7
6.2
(b)
$a_2(x,t=13)$
0
-13
0
+13
17
(c)
$a_2(x,t=16)$
0
-16
0
+16
34
(d)
$a_2(x,t=20)$
0
-20
0
+20
X
XBL757-3361

Fig. 26

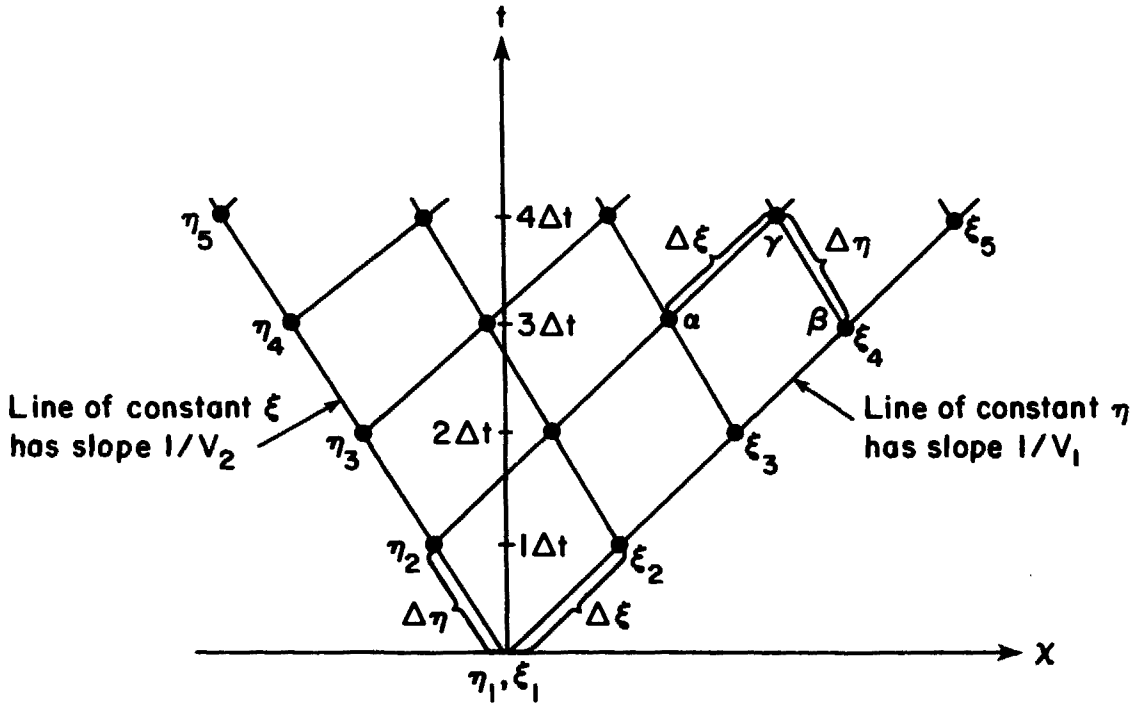

XBL757-3353

Fig. 27